ATTENUATION OF REPEATED SHOCK WAVES IN TUBES

HAROLD L. CARPENTER
AND
ROBERT W. BAUMAN

ATTENUATION OF REPEATED SHOCK WAVES IN TUBES

* * * * *

Harold L. Carpenter

and

Robert W. Bauman

ATTENUATION
OF
REPEATED SHOCK WAVES
IN
TUBES

by

Harold L. Carpenter

Lieutenant Commander, United States Navy

and

Robert W. Bauman

Lieutenant Commander, United States Navy

Submitted in partial fulfillment of
the requirements for the degree of

MASTER OF SCIENCE
IN
PHYSICS

United States Naval Postgraduate School
Monterey, California
1 9 5 9

ATTENUATION OF REPEATED SHOCK WAVES IN TUBES

by

Harold L. Carpenter
and
Robert W. Bauman

This work is accepted as fulfilling

the thesis requirements for the degree of

MASTER OF SCIENCE

IN

PHYSICS

from the

United States Naval Postgraduate School

ABSTRACT

In this investigation repeated shock waves of frequencies from 450 to 950 cycles per second were propagated in five cylindrical tubes of different inside diameters ranging from 3/4 inches to 2 3/4 inches. Amplitude of the shock waves was measured with a calibrated Altec 21-BR-200 microphone fitted with a special probe. Attenuation of the shock waves in the tubes was measured by comparison of amplitudes and wave forms at successive distances along the tube with those of a designated reference station.

The experimental results show dependence of attenuation on tube radius, pressure and frequency. The experimental evidence supports Rudnick's theory for the attenuation of guided repeated shock waves when the shock characteristic term is corrected to agree with Fay's analysis.

The writers desire to express their sincere appreciation to Professor H. Medwin of the U. S. Naval Postgraduate School for his assistance and encouragement in this investigation.

TABLE OF CONTENTS

LIST OF ILLUSTRATIONS

LIST OF ILLUSTRATIONS

1. Introduction.

As noted by two previous investigators[1] on this same subject there is little experimental substantiation for theorized behavior of repeated finite shock waves. This situation is more or less normal for all new fields of investigation. One method of attacking the problem is to increase the amount and accuracy of experimental data under all possible conditions. Then by analysis and correlation of results a behavior pattern or patterns may become evident. This investigation was geared to the above mode of attack with the purpose of extending and adding to present knowledge on the subject of repeated finite shock waves. Specifically the authors were concerned with the attenuation of repeated shock waves down tubes, what behavior the attenuation exhibited, and whether this behavior was capable of being explained by existing theory.

The investigation of shock waves in confined channels takes on a real significance in dissipation of high noise levels at low frequencies.[1] Of more basic importance, perhaps, is the fact that a confined channel (such as a cylindrical tube) provides an ideal means of studying the repeated shock wave and obtaining experimental data. It is easily instrumented and handled. Furthermore with the development of adequate theory the behavior of the repeated finite shock wave in a

[1]Anderson and Mehrtens, Attenuation of Repeated Shock Waves in Tubes, U. S. Naval Postgraduate School, Monterey, Calif., 1958

tube can be extended to other types of repeated shock waves (spherical, infinite plane, etc.).

2. Characteristics of repeated shock waves. [2]

Unlike single shock waves (as generated by explosions, nuclear blasts, etc.) which propagate with greater than acoustic velocity, repeated shock waves travel with approximately the normal speed of sound. The repeated shock wave has a sawtooth wave form (shown in Fig. 12). The shock wave form is stable except for a gradual attenuation in amplitude as it progresses further from its source (this progressive attenuation is shown in Fig. 15).

The sawtooth form of the shock wave is produced by distortion of a large amplitude sound wave. If the wave has sufficient amplitude, it will develop into a shock wave regardless of its initial form. This is due to the fact that the crest of the sound wave travels at greater velocity than the trough. The initial wave form progressively distorts finally becoming a sawtooth wave at which point the shock front is fully developed. This process is shown in Fig. 1 for an initial sine wave form.

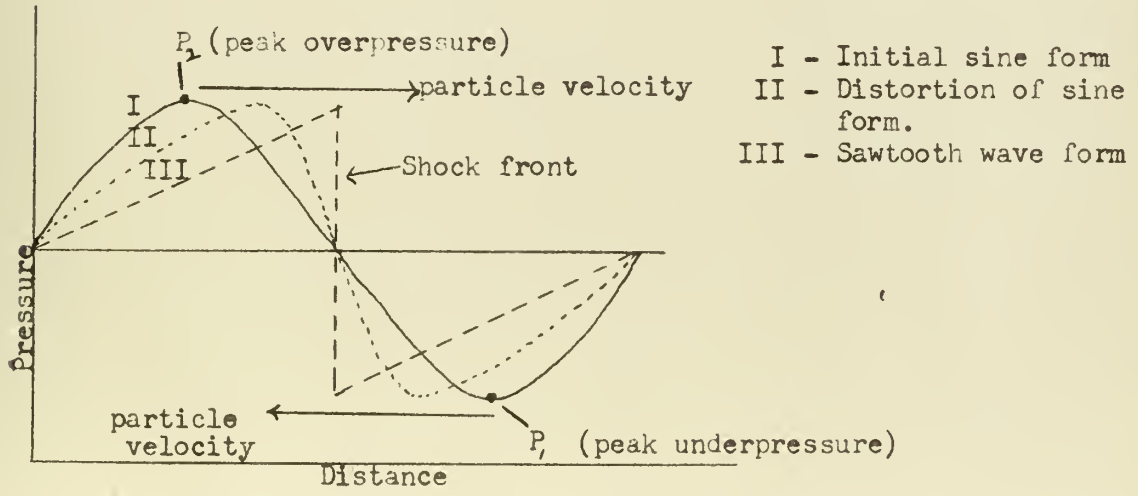

Figure 1. Development of Sawtooth Wave

The distortion of a high amplitude sound wave into a shock wave can easily be observed using a pressure sensitive probe or microphone and an oscilloscope to detect the sound wave as it is propagated down a tube. At the beginning of the tube the normal sound wave is observed; further along the tube the sound wave form becomes distorted in the direction of a sawtooth form; finally, at some further portion of the tube the shock front is fully developed and a sawtooth wave form is observed.

The primary characteristic of the shock wave form is its stability. It will not change form if it is a true shock and the only change it shows is a decrease in amplitude due to attenuation.

3. Theories on the attenuation of repeated shock waves.

Professor I. Rudnick [2] using the Rankine-Hugoniot relations has equated the entropy gain across the shock front to the decrease of energy and developed the following formula for the attenuation due to the shock characteristics of the wave:

$$\frac{1}{\delta}\frac{d\delta}{dx} = -\frac{\gamma+1}{2\gamma}\frac{\delta}{X} \qquad (1)$$

Which when integrated using $\delta = \delta_0$ at $X = 0$ becomes:

$$\frac{1}{\delta} - \frac{1}{\delta_0} = \frac{\gamma+1}{2\gamma}\frac{X}{\lambda} \qquad (2)$$

where $\delta = \frac{P_2 - P_1}{P_1}$

$\delta_0 = \left(\frac{P_2 - P_1}{P_1}\right)_{X=0}$

$\gamma = \frac{C_p}{C_v}$

λ = wave length

X = distance from reference point

The important assumptions made in the derivation are: (1) the form of the repeated shock wave is a sawtooth, (2) the wave retains its form during attenuation and (3) the entropy change occurs only at the discontinuous part of the wave. Since the above equation is one dimensional, an infinite plane wave is implied.

R.D. Fay [7] using the classical forms of the continuity equations, developed for plane sound waves of finite amplitude the following expression:

$$p = P_0\left(\frac{2\gamma}{\gamma+1}\right)\left(\frac{4M\omega}{S_0^2}\right)\sum_{n=1}^{n=\infty}\frac{\sin\left(\omega t - \frac{\omega X}{S_0}\right)}{\sinh n(\alpha_0 + \alpha_n)} \qquad (3)$$

where $M = \frac{4\mu}{3\rho_0}$

μ = coefficient of viscosity

ρ = density

P = total pressure

p = excess pressure

X = distance from the plane of ref.

S = speed of propagation

Rudnick [2] observed that the factor four is in error, the correct value being two. He further showed that for values of δ to the order of approximately .03, Fay's equation can be reduced to equation (1). Fay [8] has found a discrepancy in equation (3) due to the failure of including in the classical forms of the continuity equations a term accounting for the rate of change of the speed of propagation of the wave. The effect of this discrepancy would be to revise Rudnick's equation to:

$$\frac{1}{\delta} - \frac{1}{\delta_0} = \frac{\gamma+1}{3\gamma}\frac{x}{\lambda} \qquad (4)$$

The preceding theories derive an expression for attenuation due only to shock characteristics and ignore boundary conditions. No adequate theory is available to explain the attenuative processes of a contained repeated shock wave. For a small amplitude sine wave propagated in a tube of radius R it is known that attenuation is due mainly to wall effects and follows the relation: $\frac{d\delta}{\delta} = a_w dx$

where $a_w = (\pi/\mu)^{\frac{1}{2}}\left[\frac{1}{\gamma^{\frac{1}{2}}} + \frac{\gamma-1}{\gamma}\left(\frac{k}{C_v\mu}\right)^{\frac{1}{2}}\frac{1}{R}\left(\frac{f}{\rho}\right)^{\frac{1}{2}}\right]$

and for air

$$a_w \cong \frac{2.8 \times 10^{-5}}{R}\sqrt{f}$$

where k = thermal conductivity coefficient

R = radius

f = frequency (in cps)

Rudnick [3] assumed that the harmonics of the sawtooth wave would be attenuated at the tube walls by viscous and heat losses in the same manner as the small amplitude sound wave and derived the following expression for wall attenuation:

$$\frac{d\delta}{\delta} = a_2 dx \qquad (5)$$

where

$$a_2 = a_w \frac{\sum_{n=1}^{n=\infty} n^{-\frac{3}{2}}}{\sum_{n=1}^{n=\infty} n^{-2}} = 1.57\, a_w$$

$$= \frac{4.41 \times 10^{-5}}{R}\sqrt{f} \quad \text{for air}$$

He further assumed the attenuative effects due to the shock character and wall are additive which gives the equation:

$$-\frac{d\delta}{dx} = a_2\delta + a_3\delta^2$$

which when integrated using $\delta = \delta_0$ at x=o reduces to:

$$\frac{1}{\delta} - \frac{1}{\delta_0} = \left(\frac{a_3}{a_2} + \frac{1}{\delta_0}\right)\left(e^{a_2 x} - 1\right)$$

where $a_3 = \frac{\gamma+1}{2\gamma\lambda}$ or if Fay's work is correct, $a_3 = \frac{\gamma+1}{3\gamma\lambda}$

4. Prior investigations.

Prior experimental work on attenuation of repeated shock waves in tubes includes the investigations of Rudnick [3], Werth [4], Wilson and Bies [5], and Anderson and Mehrtens [6].

Rudnick generated high amplitude sound waves by means of a siren and the air supply from two aircraft engine superchargers.[2] The sound waves were propagated down a 60 foot section of pipe with 10 inch inside diameter. Frequencies of 20 to 200 cycles per second were investigated. Using the formula (see Section 3)

$$\frac{1}{\delta} - \frac{1}{\delta_0} = \frac{\gamma+1}{2\pi\lambda}(x - x_0)$$

a graph of $\frac{1}{\delta}$ vs. x was plotted. The theoretical slope of such a plot should be $\frac{\gamma+1}{2\pi\lambda}$. However, actual data yielded slopes between 50% to 100% of the theoretical value. Most slopes observed were about 70% of the theoretical value.

Werth, using equipment similar to Rudnick's, investigated repeated shock waves in one inch diameter tubes and one and one half inch diameter tubes over a frequency range of 300 to 1200 cycles per second. Werth's results were in general agreement with Rudnick's theory of attenuation and he suggested that exact agreement might be possible if there were no molecular processes or tube effects present.

[2] Report No. 45, Technical Report No. 2 on High Amplitude Sound Abatement Research Program for ONR, Soundrive Engine Co., Los Angeles, Calif., Oct. 1952

Wilson and Bies used the experimental set up of Rudnick with a five inch tube instead of a ten inch tube. Their investigation was conducted over a frequency range of 40 to 180 cycles per second and at pressure amplitudes of about 0.1 atmosphere. From their experimental results Wilson and Bies found that $\frac{1}{\delta}$ was linearly dependent on number of wave lengths down the tube but that the ratio of observed to theoretical slope varied from 0.62 to 2.08. Furthermore, there appeared to be no simple dependence on tube radius.

Anderson and Mehrtens using equipment identical, except for minor modifications, to that used in the present investigation and plotting $\frac{1}{\delta}$ vs. X showed frequency dependence of attenuation. These investigators changed the form of Rudnick's equation slightly to

$$\frac{1}{\delta} - \frac{1}{\delta_0} = \frac{\gamma+1}{2\gamma}\left(\frac{x-x_0}{\lambda}\right)$$

and plotted $\frac{1}{\delta}$ vs. $\frac{X}{\lambda}$ expecting a linear function with a constant slope of $\frac{\gamma+1}{2\gamma}$. However, the actual slopes, while linear, continued to vary with frequency. Anderson and Mehrtens then used the Rudnick equation[3] and evolved the expression

$$(R-1)\sqrt{f} = \frac{1}{\delta_{AVE.}}\,\frac{170\sqrt{V'}}{d}\,\frac{2\gamma}{\gamma+1}$$

where

$$R = \frac{\frac{1}{\delta} - \frac{1}{\delta_0}}{\frac{x-x_0}{\lambda}}\,\frac{2\gamma}{\gamma+1} = \frac{\text{Observed slope}}{\text{Theoretical plane wave slope}}$$

[3] I. Rudnick, Report No. 48, Technical Report No. 3 on High Amplitude Sound Abatement Program for ONR, Soundrive Engine Co., Los Angeles, Calif., Aug. 1954

Plotting $(R-1)\sqrt{f}$ vs. $\frac{1}{\delta_{AVE.}}$ was expected to yield a straight line of slope $\frac{170\sqrt{\nu}}{d}\,\frac{2\gamma}{\gamma+1}$. However, the actual data did not yield such slopes and it was concluded that Rudnick's equation does not adequately describe attenuation of repeated shock waves down tubes. Results did show increase in attenuation with decrease in tube radius. It was also noted that the ratio of observed to theoretical slope decreased to a certain value of frequency and then increased again.

5. Description of equipment.

The equipment used to produce the required high intensity sound waves was essentially that of Anderson and Mehrtens[4]. A compressor produced a flow of compressed air which was cut by a rotary chopper driven by an electric motor and mounted on a plate with four ports cut in it. These ports were alternately closed and opened by the chopper blades producing alternate condensations and rarefactions of air in an adjustable standing wave chamber. The repeated condensations and rarefactions produced the high intensity sound waves. By adjusting the length of the standing wave chamber a maximum pressure swing at the entrance of the propagation tube was assured. The shock wave developed down the propagation tube at a distance dependent on pressure swing and frequency. An adjustable exhaust pipe fitted to the standing wave chamber permitted minimization of the DC air flow so that the primary effect in the propagation tube was AC flow.

The five propagation tubes were twenty foot seamless steel tubes with wall thickness of 1/8 inch and inside diameters of 3/4 inch, 1 1/4 inches, 1 3/4 inches, 2 1/4 inches and 2 3/4 inches. These tubes were fitted with a flange plate at the upstream end by means of which they were bolted to the standing wave chamber. A terminal absorbing section was fitted to the downstream end of the propagation tube. Unlike that of Anderson and Mehrtens the termination was a straight

[4]Section 5, Anderson and Mehrtens, op. cit.

eight foot section of tube of the same diameter as the propagation tube. The termination contained a wedge of glass fiber absorber (Owens-Corning "Fiberglas" PF 615) with the small end at the juncture of the termination and the propagation tube. This arrangement (see Fig. 2) presented a gradually changing cross section to the shock wave so as to produce maximum absorption and minimum reflection of the shock wave.

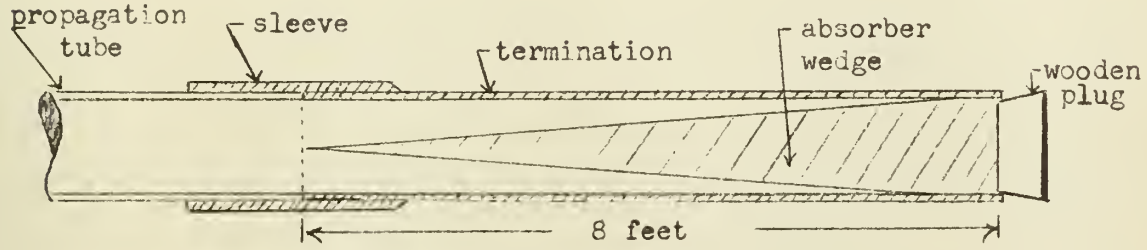

Figure 2. Diagram of Propagation Tube and Termination

The end of the termination was closed with a wooden plug to minimize possibility of DC air flow in the propagation tube.

The terminations were checked to determine the amount of reflection in the following manner. The terminations were connected to a short length of propagation tube. A loud speaker was used to propagate a signal in the tube and a travelling microphone was used to determine response at various distances (see Fig. 3).

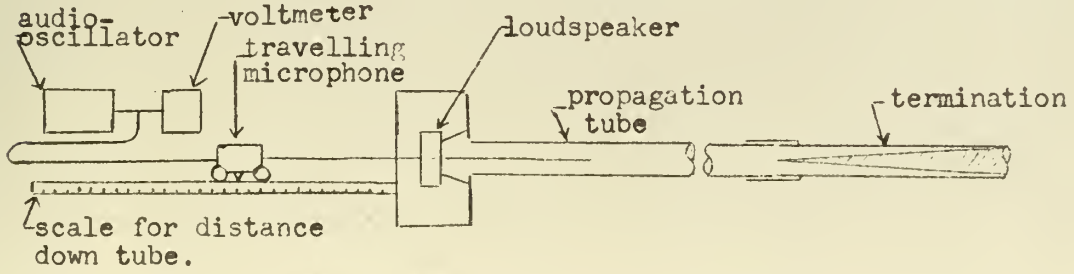

Figure 3. Termination Testing Apparatus

Absorber wedges were tailored to produce minimum reflections (i.e. maximum absorption) as determined by the microphone response. The optimum terminations showed very small standing waves. Fig. 4 shows some typical variations in response due to standing waves. It was anticipated that at experimental sound levels the absorption characteristics of the termination would be different due to a change in acoustic resistance of the glass fiber absorber. (i.e. an optimum termination for infinitesimal sound would not be optimum for the input shock). However, it was considered that the standing waves produced would not interfere with the observation of repeated shock attenuation and that any error introduced could be suitably taken into account.

The propagation tubes had threaded probe holes (1/8 inch in diameter) at one foot intervals down the length starting at four feet from the upstream end. The microphones used were fitted with probes threaded to fit these holes so that the probe end was flush with the inside tube surface.

Two microphones were used. One, an Altec 21-BR-180, monitored the input intensity of the shock wave. The other (hereafter referred to as the travelling microphone) was an accurately calibrated Altec 21-BR-200 fitted with a special probe designed to give an essentially flat response out to approximately the tenth harmonic of the highest fundamental frequencies used. Each of these microphones was used with an Altec 165A Base (containing pre-amplifier) and an Altec 526B

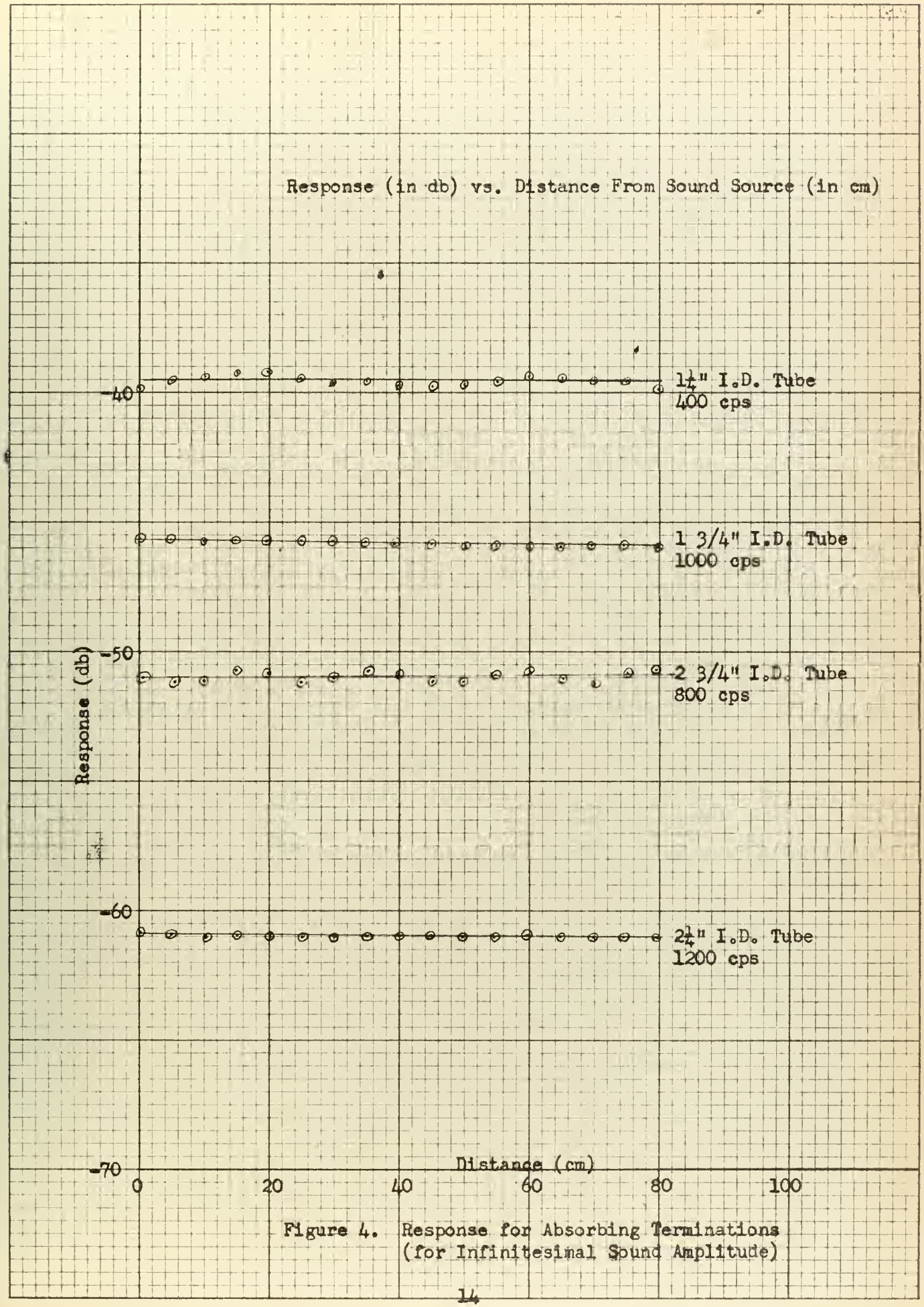

Figure 4. Response for Absorbing Terminations (for Infinitesimal Sound Amplitude)

Power Supply.

A barium titanate transducer was used just upstream of the reference station to verify existence of a shock prior to making experimental runs. This transducer was inserted through a one-fourth inch threaded hole which was plugged during the actual runs.

Two Hewlett-Packard 400D voltmeters were used to read the response of the monitor and travelling microphones. A Tektronix Dual Trace Oscilloscope (Type 545) was used to observe and match wave forms and to get initial peak-to-peak pressure at the reference station. A Decade Attenuator (General Radio Co. Type 1450-TB) graduated in 0.1 db. steps was used in the travelling microphone circuit to provide accurate and easily read attenuation values. By matching its input and output impedance the attenuator characteristics were such that it provided linear attenuation over a 100 kc. frequency range.

To control frequency of the sound wave the chopper shaft was fitted with a steel disk having nine equal sized circular holes spaced equidistantly around its periphery. A wound permanent magnet was so placed that the disk periphery rotated between the poles causing a fluctuation of current in the windings nine times per revolution. The magnet output was plotted against an oscillator output in an oscilloscope. Thus a set frequency on the oscillator could be matched by varying the chopper frequency until a Lissajou circle was observed on the oscilloscope. This arrangement permitted accurate frequency adjustment and

insured that observations were made at the proper time. For ease of frequency reading a Hewlett-Packard Electronic Counter (Model 521A) was used to count the oscillator frequency.

A schematic diagram of the experimental setup is shown in Fig. 5. The compressor, chopper and wave chamber were housed and sound-proofed to make working conditions tolerable.[5]

[5] Figs. 7 and 8, p.12, Anderson and Mehrtens, op. cit.

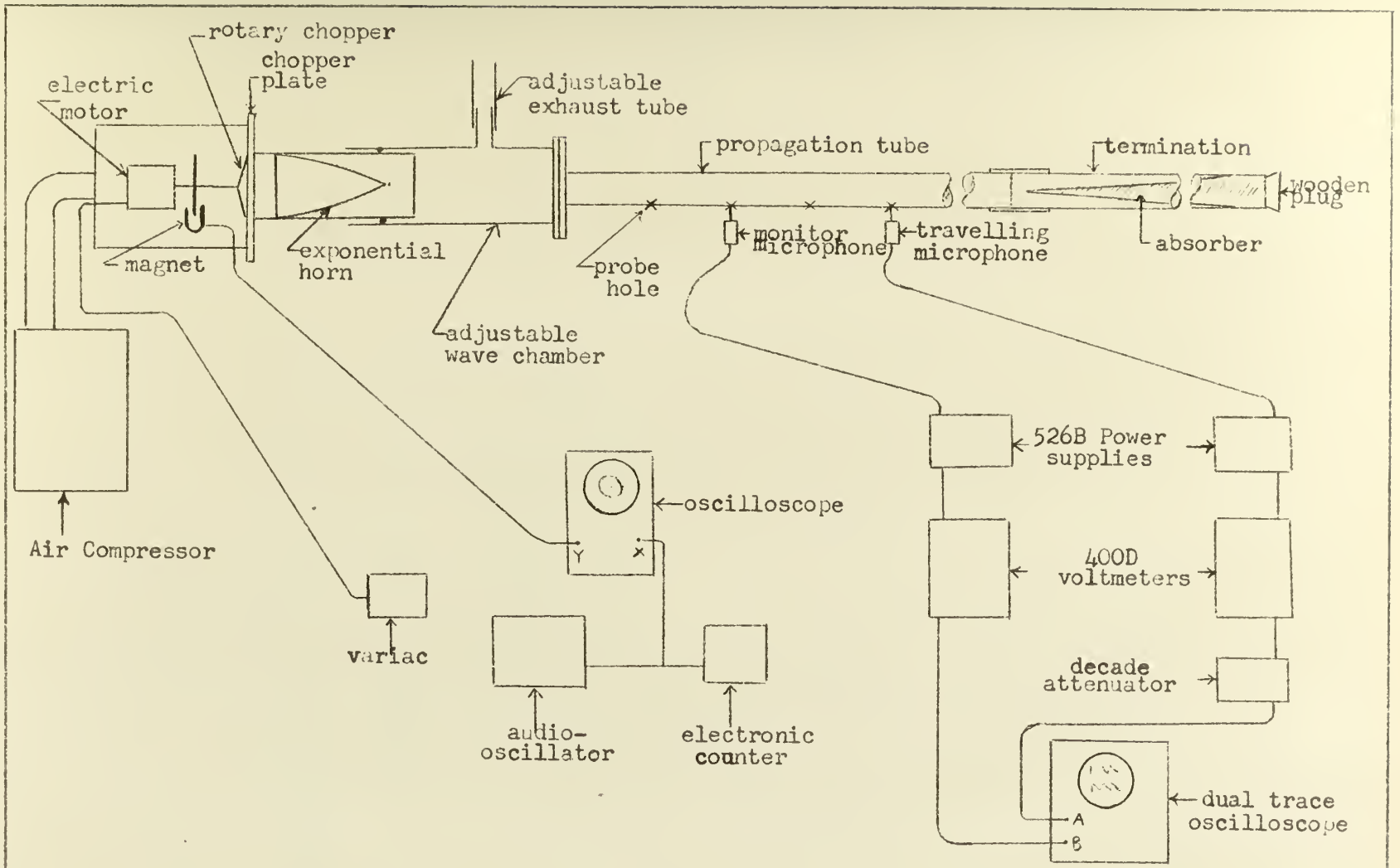

Figure 5. Schematic Diagram of Experimental Set-up

6. Design of probe adapter for Altec Microphone and absolute calibration of the microphone system.

The Altec system was chosen over the barium titanate system frequently used in high intensity sound studies because of its insensitiveness to mechanical vibrations and its ruggedness. However, the method of measuring the sound pressure through small 1/8 inch holes in the propagating tubes placed severe design criteria on the probe tube adapter. The small tube opening would greatly increase the acoustical reactance of the pick-up system and thus give a non-linear response. A linear response over as wide a frequency range as possible was needed to prevent undue distortion of the sawtooth wave. The basic design of the probe tube adapter is shown in Fig. 6.

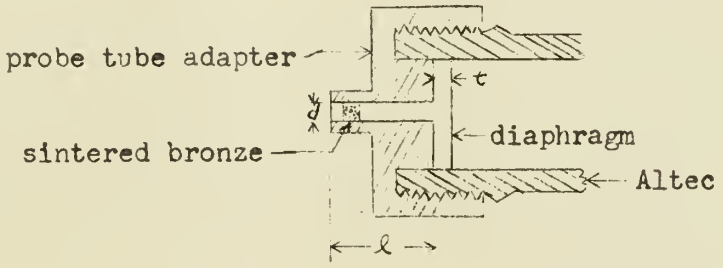

Figure 6. Basic Design of Probe Tube Adapter

Various sizes of the tube diameter (d) and the diaphragm clearances (t) were tried. From analysis of the response curves obtained, it was found that by using the acoustical circuit shown in Fig. 7 the resonant frequencies could be predicted with reasonable accuracy. A probe tube was designed on this basis which gave a linear response out to 8 kc. The dimensions of the final design were: $d = .076''$, $t = .003$

inch and ℓ = .320 inch. A sintered bronze plug 1/8 inch long was inserted in the probe tube to eliminate the resonant peaking of the microphone diaphragm and to reduce the standing wave effect on the probe tube.

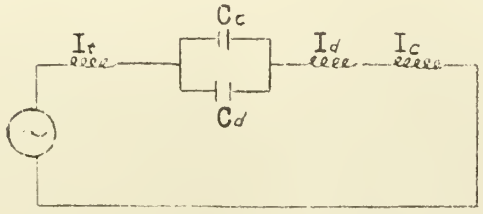

I_t - Inertance of probe tube

C_c & I_c - Compliance & inertance of cavity between plug and diaphragm

C_d & I_d - Compliance & inertance of diaphragm

Figure 7. Simplified Acoustical Circuit for Microphone and Probe Tube

The 21-BR-200 with probe tube adapter attached was calibrated using a reciprocity calibrated 640AA Western Electric Microphone as a standard. Calibration was performed in a standing wave tube of 1 inch dia. as shown in Fig. 8.

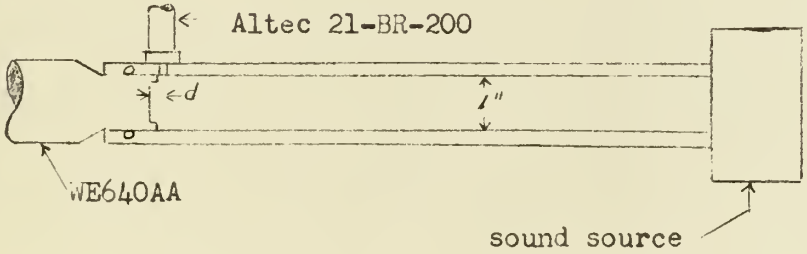

Figure 8. Microphone Calibration Tube

Frequencies above 8 kc. could not be used for calibration because of transverse modes in the tube. A correction for the axial displacement (d) was necessary and since the diaphragm of the WE-640AA does not present an infinite impedance to the sound wave this correction was not precise. The error is not significant below 4-5 kc. The response curve is shown in Fig. 9. Apparently the response decreases sharply at frequencies above 8 kc. The response curve was used to determine the coefficients of the Fourier Series terms for a sawtooth wave. Fig. 10 shows graphically the expected wave form to be reproduced by the microphone system for a sawtooth wave input of 400 cps. Comparison of Figs. 10 and 11 shows general agreement between predicted and actual wave forms reproduced.

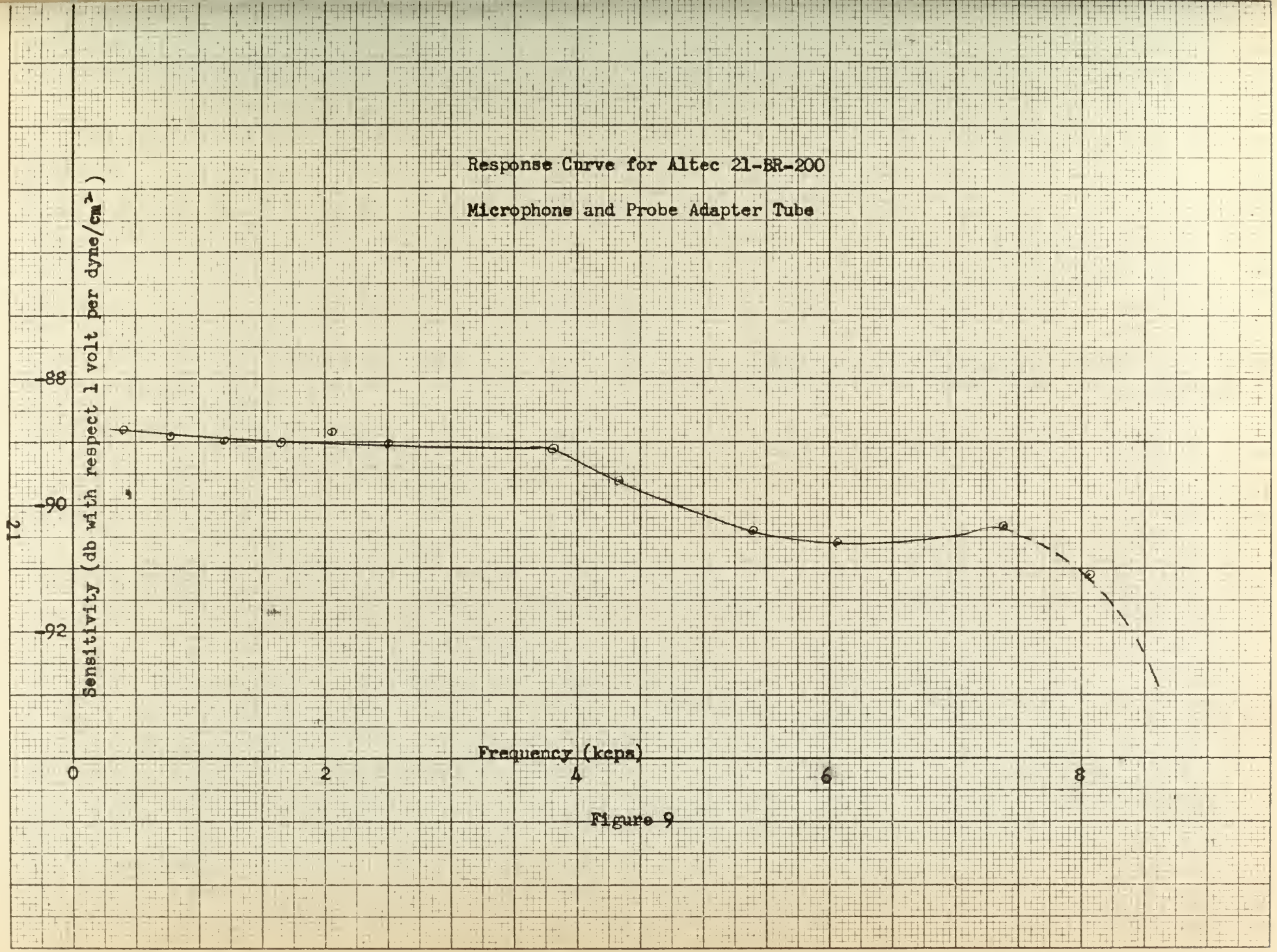
Response Curve for Altec 21-8R-200
Microphone and Probe Adapter Tube
Sensitivity (db with respect 1 volt per dyne/cm²)
-88
-90
-92
Frequency (kcps)
0
2
4
6
8

Figure 9

Predicted Wave Form of Altec Microphone

When Measuring Sawtooth Wave

$A = A_0 \sin\omega t - A_1 \frac{1}{2} \sin 2\omega t + A_2 \frac{1}{3} \sin\omega t \ldots\ldots\ldots$

A_0, A_1, A_2, etc. determined by response curve for Altec

– – – – – Completely flat response

——————— Actual response assuming sharp decrease between 8 - 9 kc. No response > 10 kc.

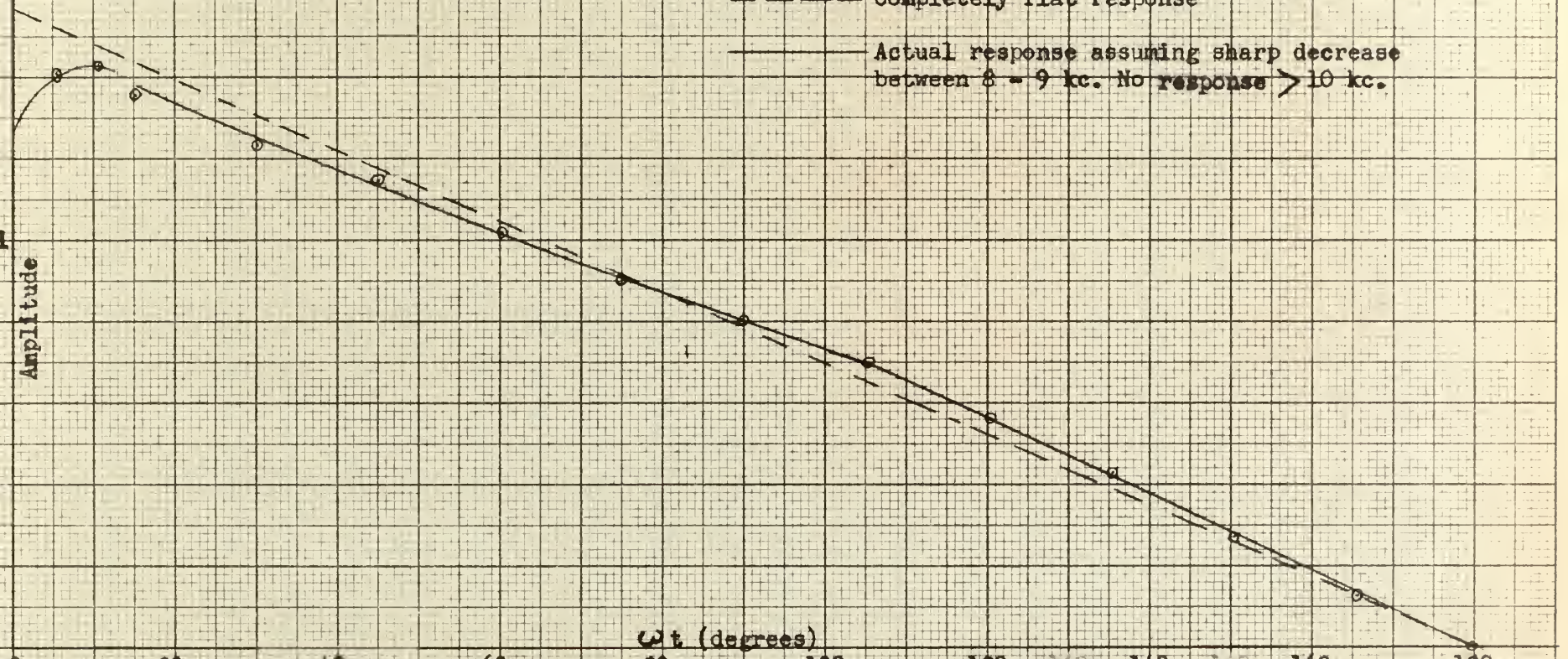

Figure 10

7. Conduct of the investigation.

Experimental data was gathered using the five propagation tubes over a range of frequencies and peak-to-peak pressures (see Section 8). The monitor microphone was located at the same station of a tube during all runs to insure a constant input intensity. This station was one foot upstream of the reference station for the travelling microphone.

Inasmuch as the travelling microphone response was not completely sawtooth in character (see Fig. 11), a barium titanate transducer (with flat response to 100 kc. or higher) was used to verify the existence of a shock wave. The transducer response leaves little doubt as to the existence of a shock wave (see Fig. 12).

Peak-to-peak pressure at the reference station was measured directly from the oscilloscope trace of the travelling microphone. This microphone's response to a shock wave differed from a true sawtooth form only in that the overpressure peak was rounded (see Fig. 11) due to suppression of the higher harmonics occasioned by the probe design and microphone sensitivity. The method used was to extrapolate the leading and trailing gradients of the travelling microphone response to an intersection point which marked the maximum overpressure point (i.e. the peak of the true sawtooth form). Then using the calibrated face of the oscilloscope the peak-to-peak voltage was measured (see Figs. 13 and 14) and converted to pressure.

After measurement of the peak-to-peak pressure the response of

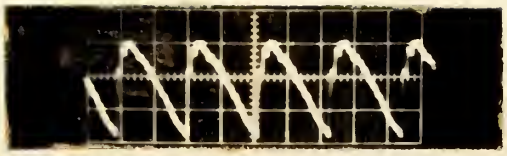

Figure 11. Oscillogram of Altec 21-BR-200 Microphone System Response to Shock Wave

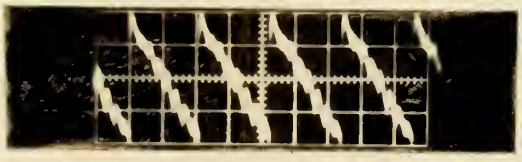

Figure 12. Oscillogram of Barium Titanate Transducer Response to Shock Wave

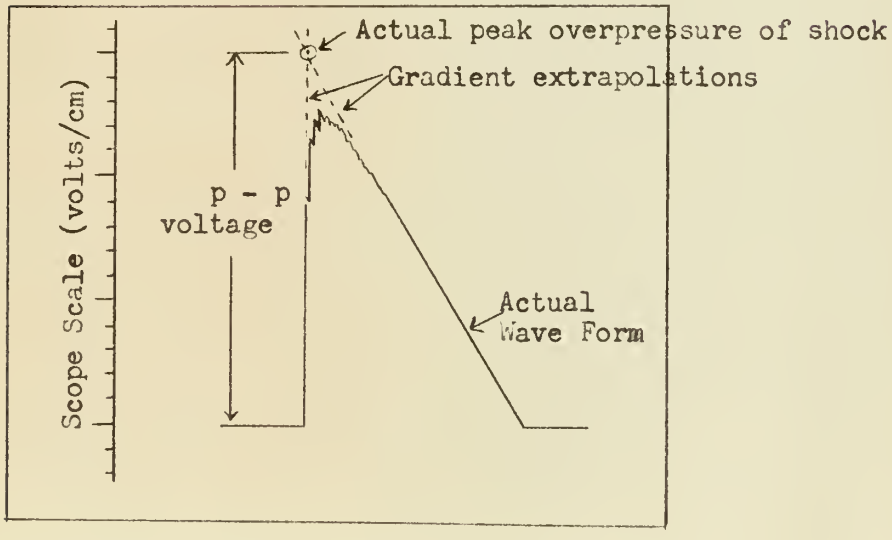

Figure 13. Determination of Peak-to-Peak Voltage on Oscilloscope

the reference station was decreased using the decade attenuator in the travelling microphone circuit. This initial attenuator reading was recorded and the decreased wave response was traced on the face of the oscilloscope. As the travelling microphone was moved to other stations downstream, the response decreased due to the shock wave attenuation. At each station this response was increased back to reference response by taking off suitable amounts of attenuation on the attenuator. The difference between attenuator readings for the reference station and any other station (balanced back to reference response) gave shock wave attenuation directly. At any station the amount of attenuation taken off the attenuator was such as to bring the travelling microphone response on the Hewlett-Packard voltmeter up to the reference station value. This could be done to an accuracy of 0.1 db. Simultaneously, the monitor voltmeter response was checked to see that it had remained constant and the wave form of the travelling microphone response was checked against the reference trace drawn on the oscilloscope face to insure that it had not changed. All readings were taken when the frequency oscilloscope showed a Lissajou circle (see Section 5) to insure that frequency was constant. Fig. 15 shows the progressive attenuation of the repeated shock wave as it proceeds down the tube.

For this investigation room temperature was 70° F., ambient pressure was 10^{6} dynes/cm^{2}, and acoustic velocity was 3.4×10^{4} cm/sec. All attenuation data were measured and expressed in decibels.

Figure 14. Oscillogram of Altec Microphone System Response Superimposed on Barium Titanate Transducer Response

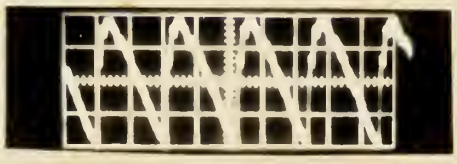

Station No. 6

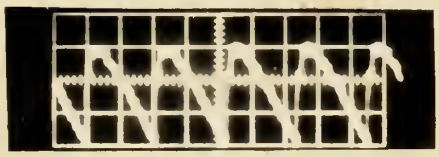

Station No. 11 (5 ft. downstream from No. 6): Amplitude $\sim$ 3/4 Amplitude at No. 6

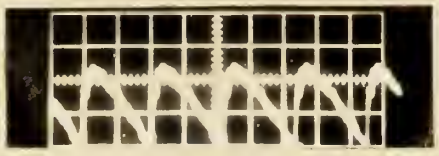

Station No. 16 (10 ft. downstream from No. 6): Amplitude $\sim \frac{1}{2}$ Amplitude at No. 6

Figure 15. Oscillograms of Progressive Attenuation of Shock Wave in Tube

8. Limits of the investigation.

Peak-to-peak pressures were measured at one foot intervals over a distance of approximately 13 feet on tubes of inside diameters of 3/4 inch, 1 1/4 inches, 1 3/4 inches, 2 1/4 inches, and 2 3/4 inches. Table 1 (Fig. 16) gives the peak-to-peak pressure and frequency ranges used with the various tubes in the conduct of the investigation. The peak-to-peak pressures listed are the values obtained at a reference station 8 feet from the pipe inlet and approximately 12 1/2 feet from the chopper. All pressure and distance measurements are based on this station as an arbitrary zero reference point.

Table 1: Experimental Frequency and Pressure Ranges

Pipe Diameter	Frequency Range (cps)	P-P Pressure Range at Ref. Pt. (Atm)
3/4"	506 - 794	0.085 - 0.214
1 1/4"	505 - 945	0.085 - 0.187
1 3/4"	443 - 912	0.178 - 0.107
2 1/4"	494 - 926	0.093 - 0.198
2 3/4"	494 - 921	0.097 - 0.224

Figure 16

9. Analysis of the data.

A. Attenuation due to shock front.

Expanding $e^{a_2 x}$ in a power series, Rudnick's equation

$$\frac{1}{\delta} - \frac{1}{\delta_0} = \frac{a_3}{a_2}\left(e^{a_2 x} - 1\right) + \frac{1}{\delta_0}\left(e^{a_2 x} - 1\right) \qquad (6)$$

becomes

$$\frac{1}{\delta} - \frac{1}{\delta_0} = \frac{a_3}{a_2}\left(a_2 x + \frac{a_2^2 x^2}{2!} + \cdots\right) + \frac{1}{\delta_0}\left(a_2 x + \frac{a_2^2 x^2}{2!} + \cdots\right)$$

Within the limits of the investigation the highest value of a_2 would be obtained in the 3/4 inch tube at maximum frequency and would be of the order of approximately .04 per foot. For maximum length of traverse (x = 12 feet) the term $a_2 x < 1$. The above equation can therefore be reduced to:

$$\frac{1}{\delta} - \frac{1}{\delta_0} = \left(\frac{a_3}{a_2} + \frac{1}{\delta_0}\right)\left(a_2 x + \frac{a_2^2 x^2}{2}\right)$$

or

$$\frac{1}{\delta} - \frac{1}{\delta_0} = \frac{x}{\lambda}\left(a_3\lambda + \frac{a_2\lambda}{\delta_0}\right) + \frac{x^2}{\lambda^2}\left(\frac{a_3 a_2 \lambda^2}{2} + \frac{a_2^2\lambda^2}{2\delta_0}\right) \qquad (7)$$

This expression implies that a plot of $\frac{1}{\delta}$ vs. $\frac{x}{\lambda}$ would produce a curved plot. Since the non-linear terms are very small within the parameters of this experiment, the curvature should be masked by the experimental errors. Fitting the best straight line to the points of a plot of the experimental values of $\frac{1}{\delta}$ vs. $\frac{x}{\lambda}$ should then yield some interesting information. The slope of the line should increase with frequency and decrease with an increase of peak-to-peak pressure input (i.e. increase with increasing $\frac{1}{\delta_0}$). Further, for any given peak-to-peak pressure input and frequency a plot of slope vs. tube diameter should reasonably be expected to approach the value $a_3\lambda$ (dependent only on the gas used)

asymptotically with increasing tube diameter.

B. Attenuation due to wall effects.

Equation (6) can also be rearranged into the following form:

$$\frac{\frac{1}{\delta} + \frac{a_3}{a_2}}{\frac{1}{\delta_0} + \frac{a_3}{a_2}} = e^{a_2 x} \qquad (8)$$

It can be seen that if $\ln(\frac{1}{\delta} + \frac{a_3}{a_2})$ is plotted against X a straight line whose slope is equal to a_2 should be obtained. With a correct value of a_3, use of an initial theoretical value for a_2 in the log term with successive approximations should converge to an experimental value of a_2. Comparison of this value with the theoretical value would give experimental evidence as to the validity of Rudnick's method of addition of wall losses due to harmonic components of the sawtooth wave. Also the interrelation of shock characteristic and wall attenuation could be assessed. This procedure has the advantage of excluding any errors in the determination of the reference peak-to-peak pressure, $\frac{1}{\delta_0}$.

10. Interpretation of data.

Data presented in Figs. 17 through 25 as graphs of $\frac{1}{\delta}$ vs. $\frac{x}{\lambda}$ does not include all of the data collected (for additional data see Appendix I). They are representative data chosen to illustrate the significant results derived from the investigation. Data not shown also substantiate these results. Displacements have been added to or subtracted from experimental values of $\frac{1}{\delta}$ and $\frac{x}{\lambda}$ for a given set of data to permit more compact illustration. If the non-linear term is neglected in equation (7), which can reasonably be done in this investigation, the slopes of lines drawn in Figs. 17 through 25 should be approximately equal to

$$a_3\lambda + \frac{a_2\lambda}{\delta_0}$$

Thus the slopes in air should depend on strength of shock, frequency, and tube diameter (through a_2). Figs. 18 and 24 show the results of data taken for 2 3/4 inches and 1 1/4 inches tube diameters at constant peak-to-peak pressures at the reference point and at various frequencies in an effort to determine frequency dependence. Fig. 24 shows increasing attenuation with increasing frequency. Fig. 18 is not conclusive, the reason being that for the limited frequency range used in the larger tube the change of slope is hidden by the experimental errors. Data shown in Fig. 23 were taken in an effort to determine dependence on initial pressure for constant frequency but the standing wave problem precluded any possibility of drawing a reliable conclusion from this data. If Figs. 17, 19, 22 and 25 are examined with care,

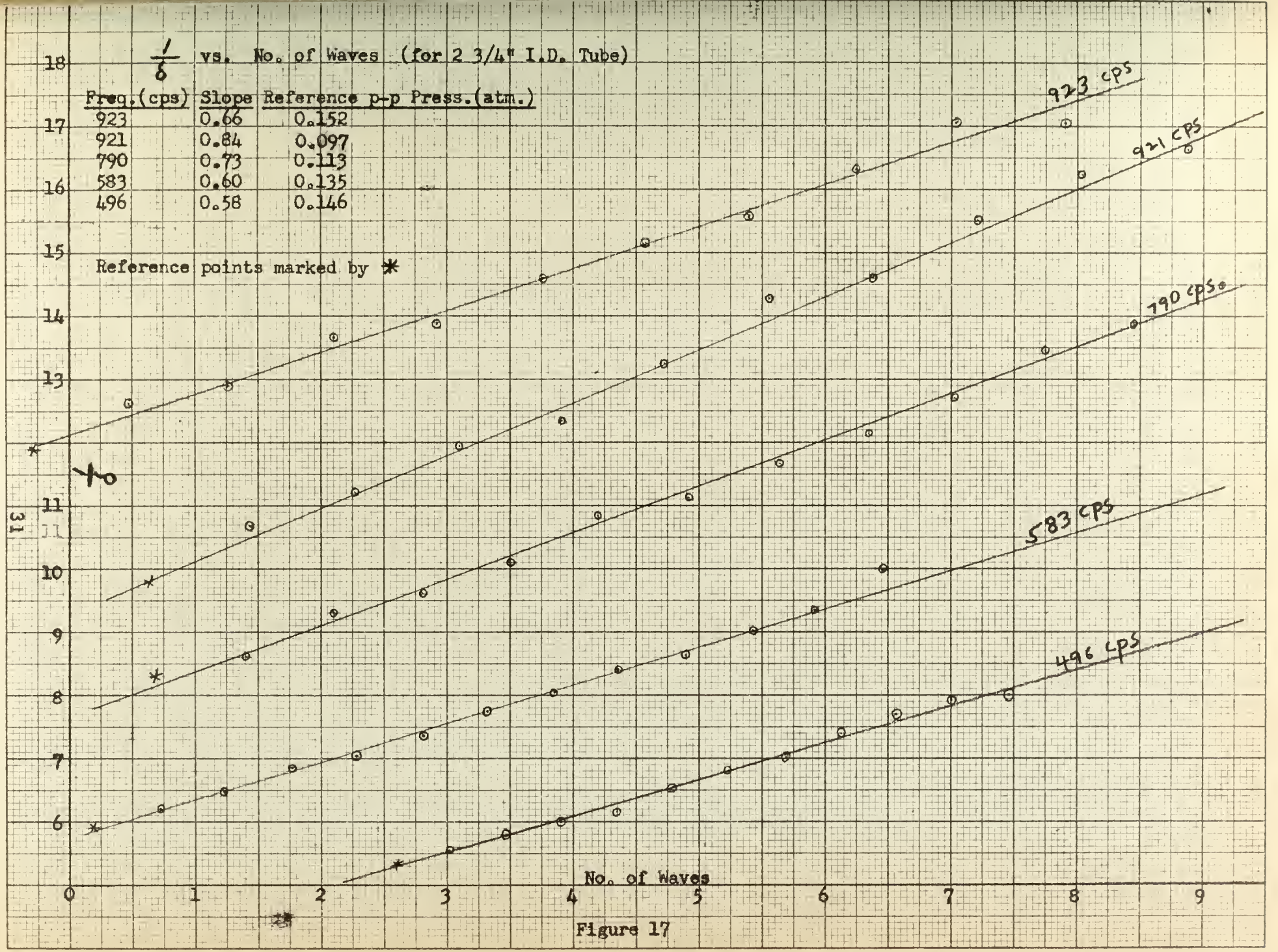
1/δ vs. No. of Waves (for 2 3/4" I.D. Tube)
Freq.(cps) Slope Reference p-p Press.(atm.)
923 0.66 0.152
921 0.84 0.097
790 0.73 0.113
583 0.60 0.135
496 0.58 0.146
Reference points marked by *
923 cps
921 cps
790 cps
583 cps
496 cps
1/δ
No. of Waves

Figure 17

$\frac{1}{\delta}$ vs. No. of Waves (for 2 3/4" I.D. Tube)

Constant p-p pressure of 0.152 atm. at reference points.

Reference points marked by *

Freq.(cps)	Slope
897	0.63
790	0.61
737	0.64
693	0.61

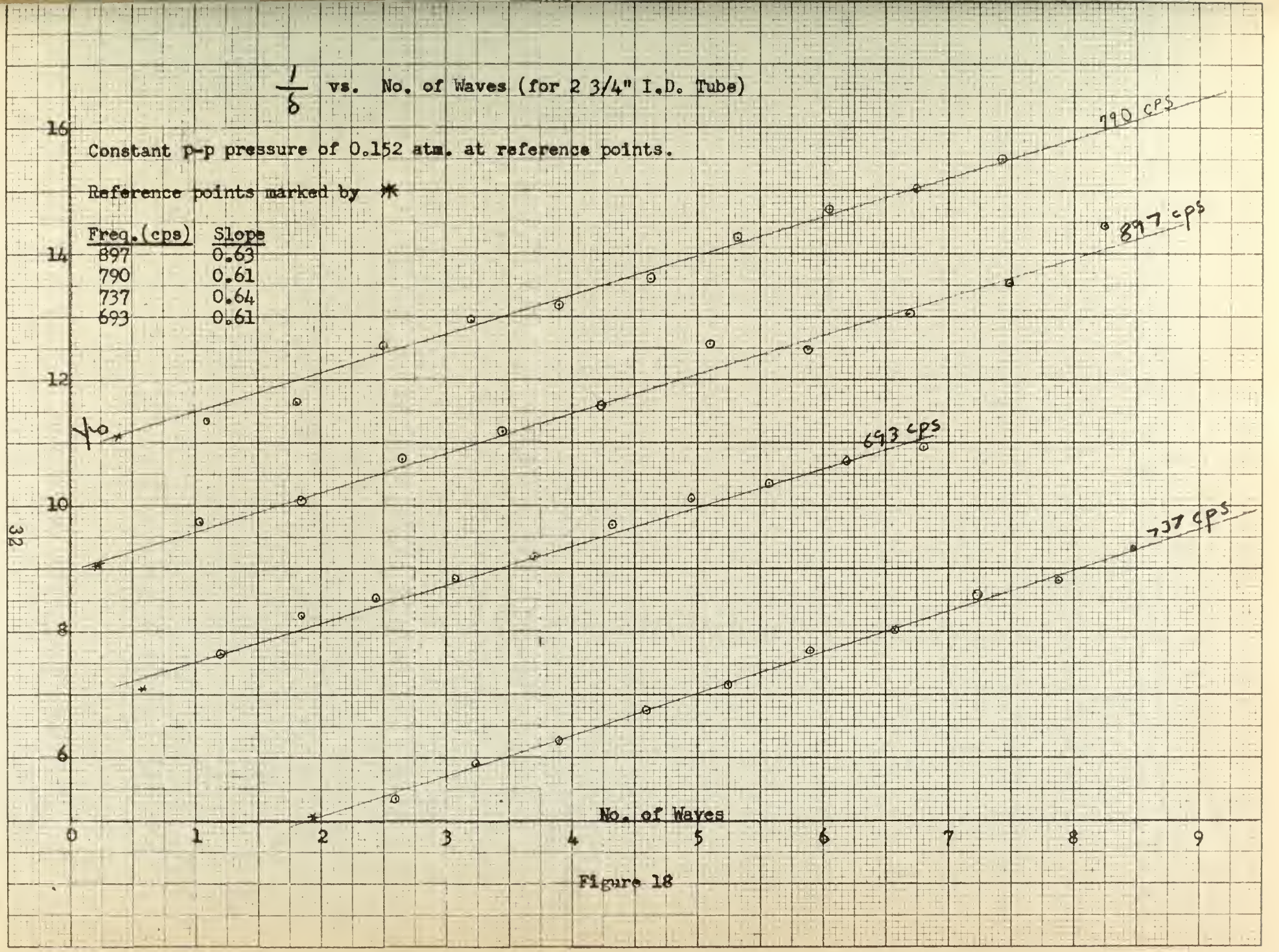

Figure 18

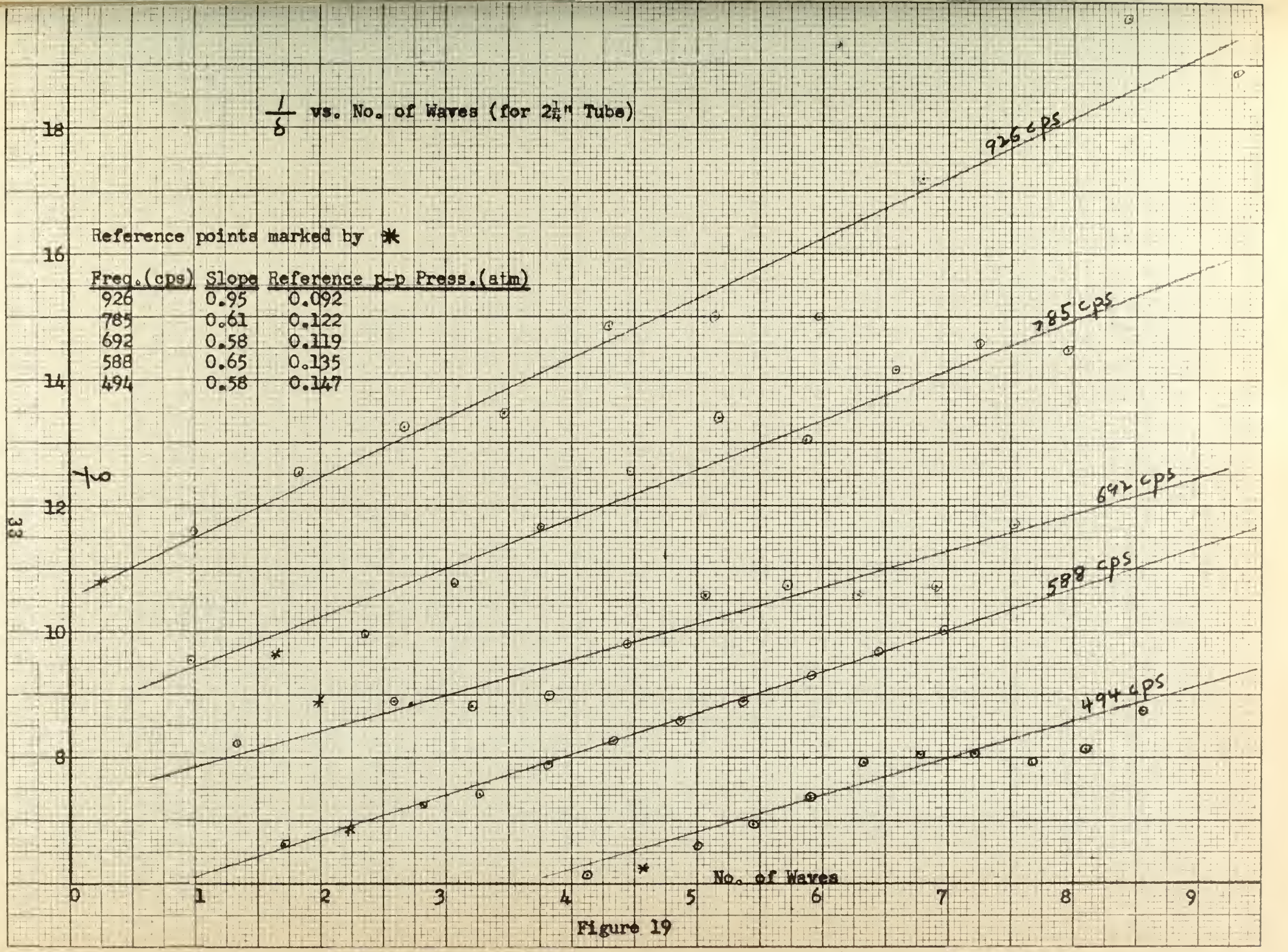
1/δ vs. No. of Waves (for 2¼" Tube)
Reference points marked by *
Freq.(cps) Slope Reference p-p Press.(atm)
926 0.95 0.092
785 0.61 0.122
692 0.58 0.119
588 0.65 0.135
494 0.58 0.147
926 cps
785 cps
692 cps
588 cps
494 cps
1/δ
No. of Waves
18
16
14
12
10
8
0
1
2
3
4
5
6
7
8
9

Figure 19

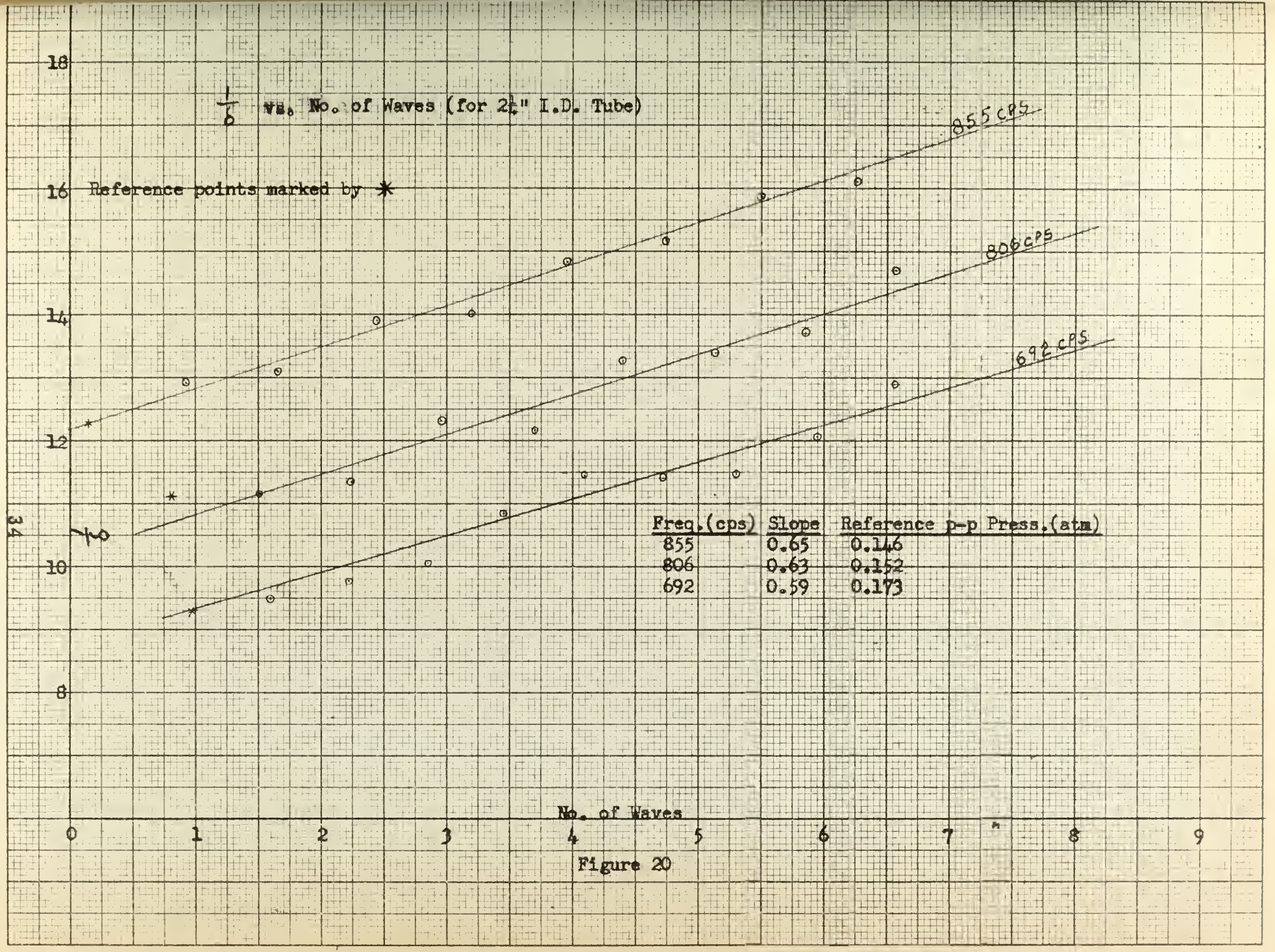

Freq.(cps)	Slope	Reference p-p Press.(atm)
855	0.65	0.146
806	0.63	0.152
692	0.59	0.173

Figure 20

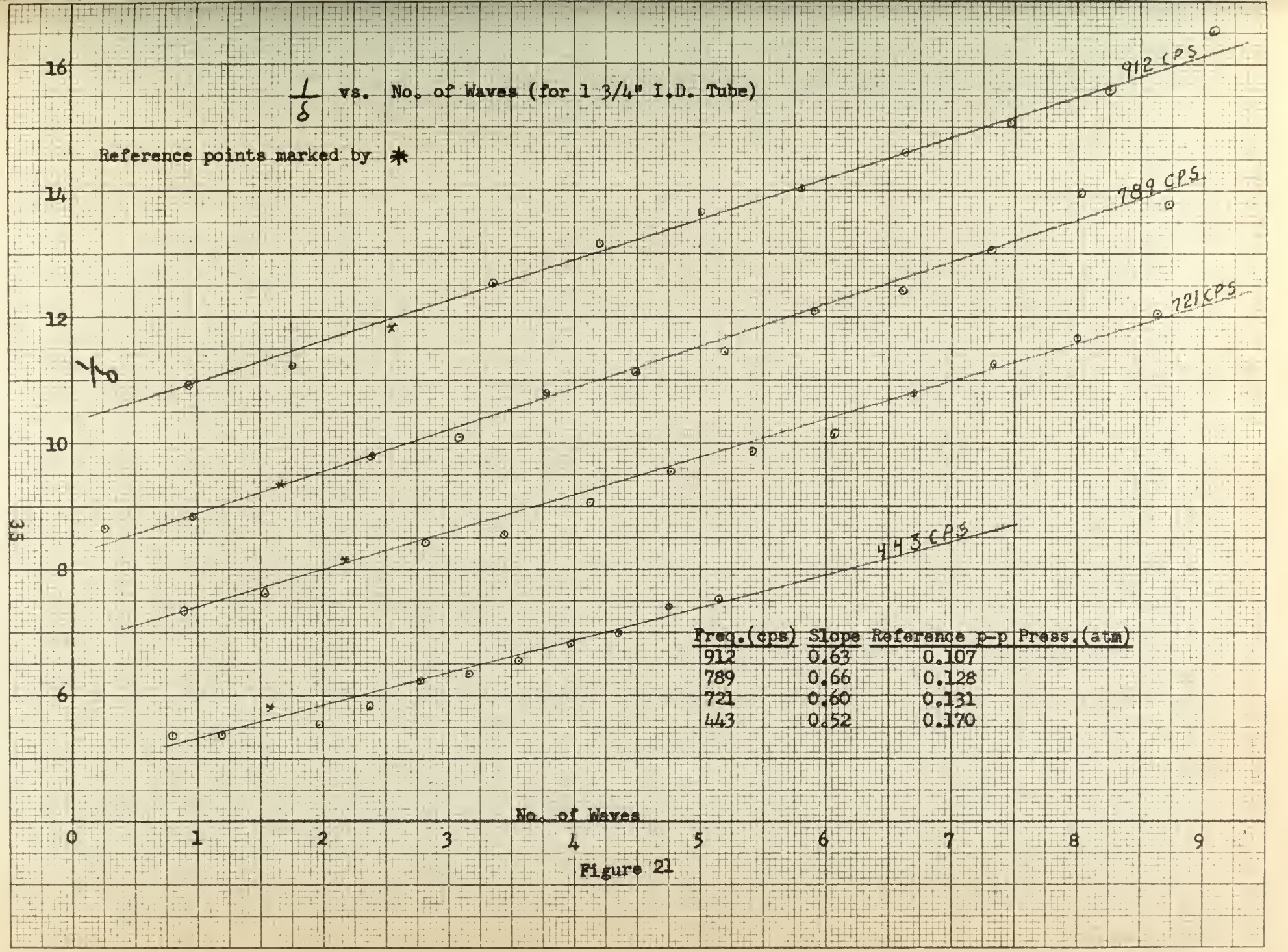

Freq.(cps)	Slope	Reference p-p Press.(atm)
912	0.63	0.107
789	0.66	0.128
721	0.60	0.131
443	0.52	0.170

Figure 21

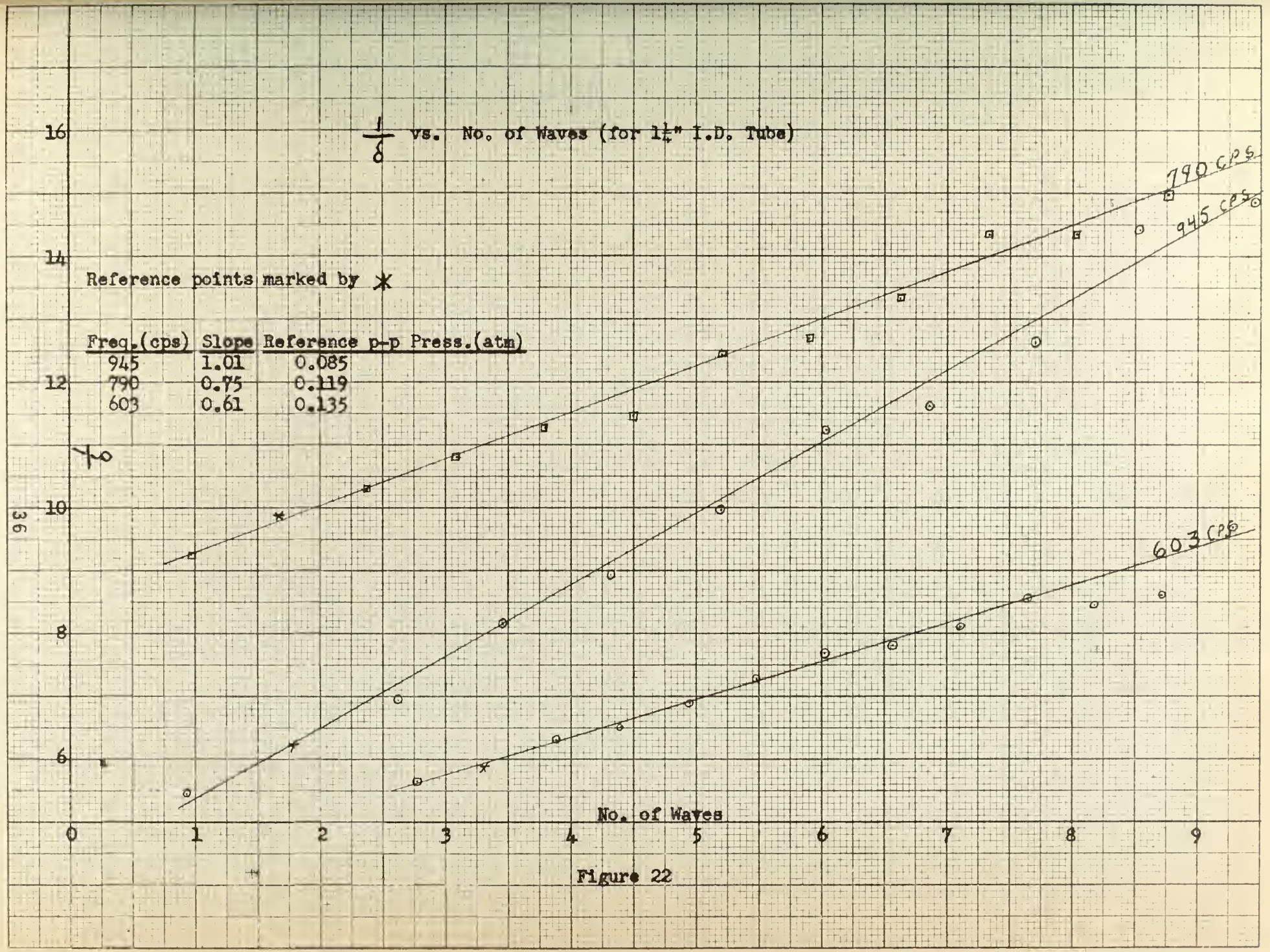
1/δ vs. No. of Waves (for 1¼" I.D. Tube)
Reference points marked by ✳
Freq.(cps) Slope Reference p-p Press.(atm)
945 1.01 0.085
790 0.75 0.119
603 0.61 0.135
1/δ
No. of Waves
790 cps
945 cps
603 cps
16
14
12
10
8
6
0
1
2
3
4
5
6
7
8
9

Figure 22

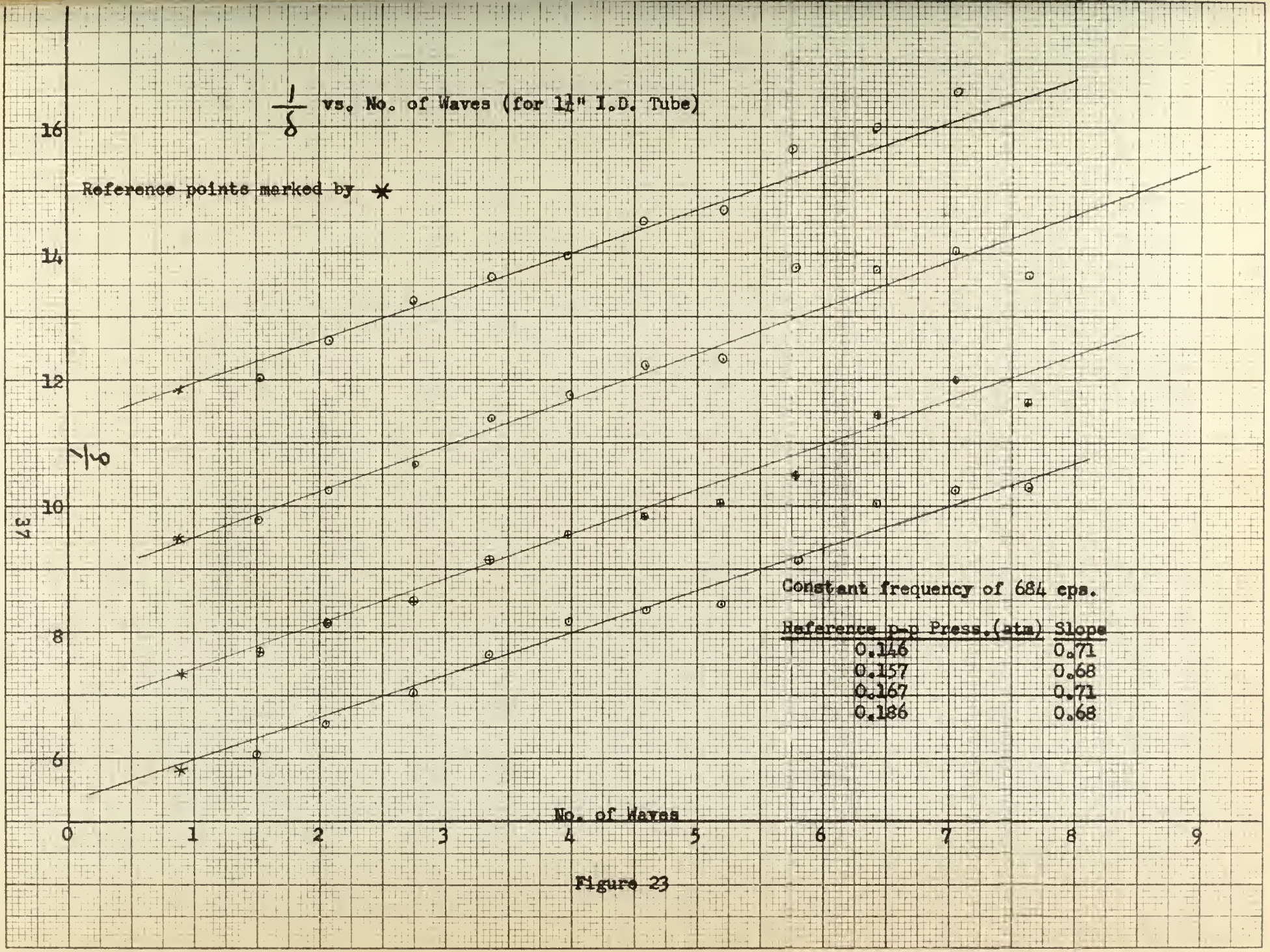
1/δ vs. No. of Waves (for 1½" I.D. Tube)
Reference points marked by ✱
1/δ
No. of Waves
0
1
2
3
4
5
6
7
8
9
6
8
10
12
14
16
Constant frequency of 684 cps.
Reference p-p Press.(atm) Slope
0.146 0.71
0.157 0.68
0.167 0.71
0.186 0.68

Figure 23

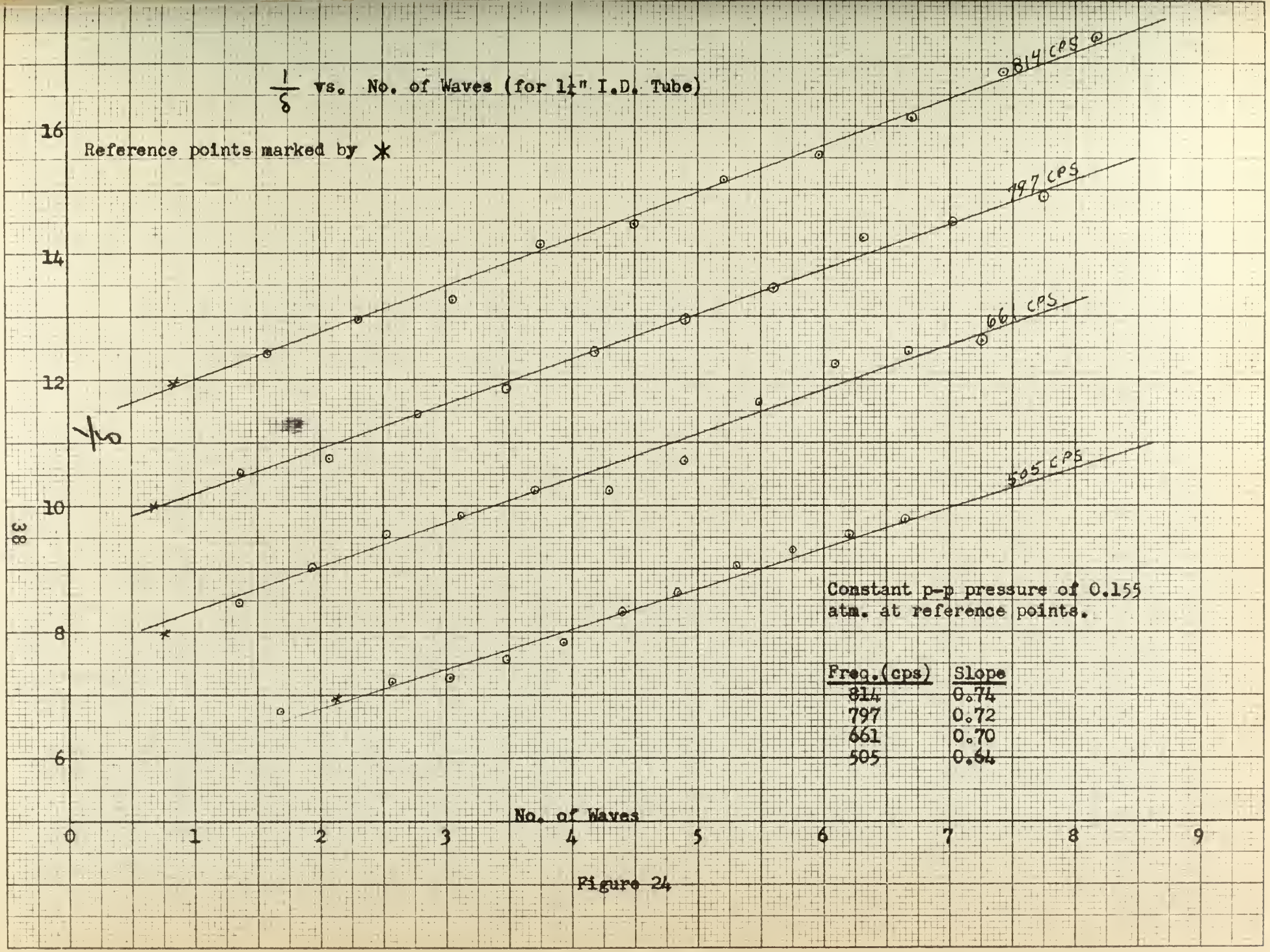

Constant p-p pressure of 0.155 atm. at reference points.

Freq.(cps)	Slope
814	0.74
797	0.72
661	0.70
505	0.64

Figure 24

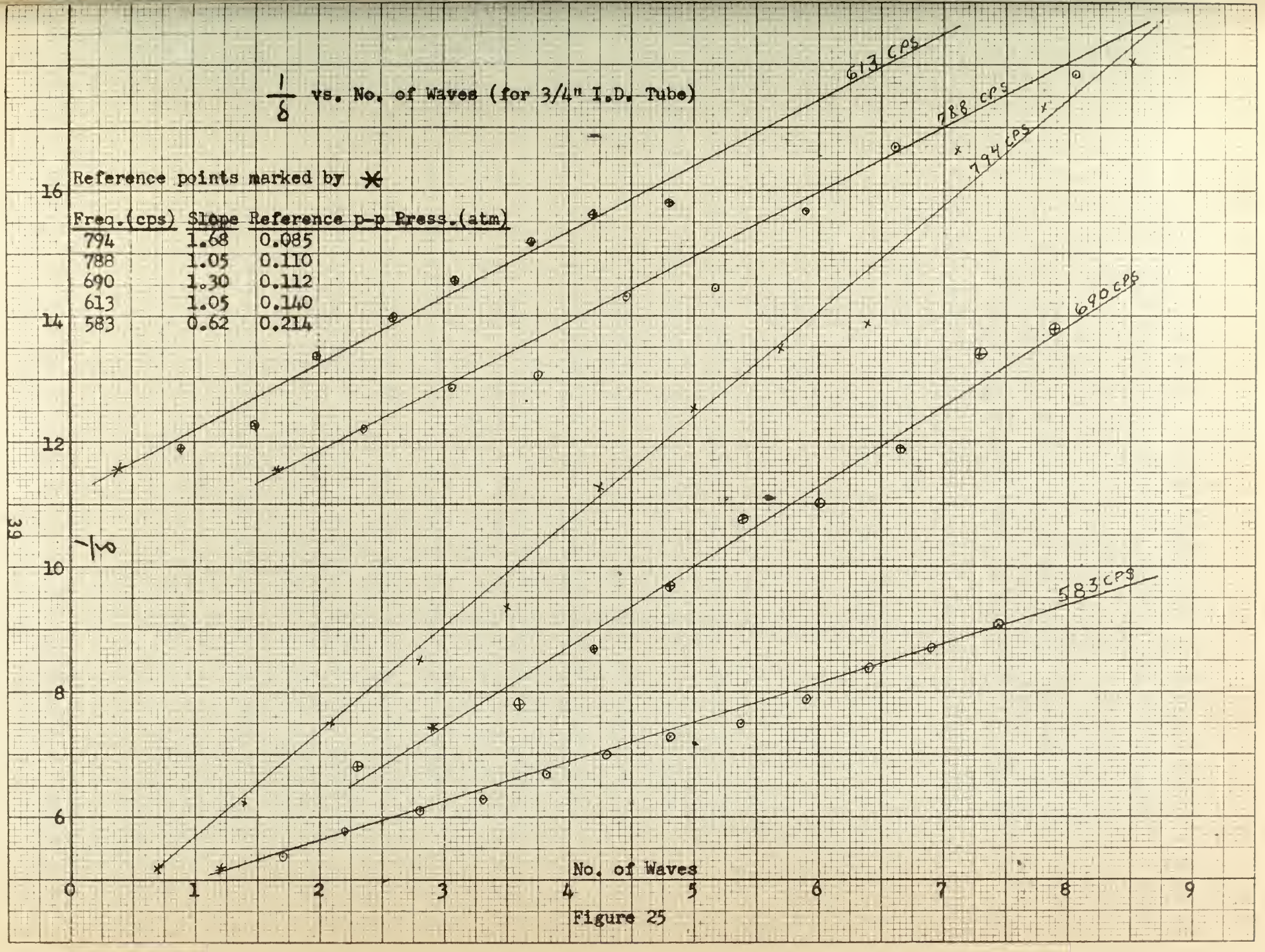
1/δ vs. No. of Waves (for 3/4" I.D. Tube)
Reference points marked by ✳
Freq.(cps) Slope Reference p-p Press.(atm)
794 1.68 0.085
788 1.05 0.110
690 1.30 0.112
613 1.05 0.140
583 0.62 0.214
613 CPS
788 CPS
794 CPS
690 CPS
583 CPS
1/δ
No. of Waves
16
14
12
10
8
6
0
1
2
3
4
5
6
7
8
9

Figure 25

pressure dependence is evident. Specifically, the variation in slopes for the 923 and 921 cps curves of Fig. 17 and for the 788 cps and 794 cps curves of Fig. 25 shows dependence on initial peak-to-peak pressure. The other curves of Figs. 17, 22 and 25 show both pressure and frequency dependence but the two effects are not yet easily separated in this raw data.

From the expression for the slope

$$\text{slope} \approx a_3\lambda + \frac{a_1\lambda}{\delta_0}$$

and assuming that

$$a_1 = \frac{k}{R}$$

it can be seen that a plot of slope vs. tube diameter, where $\frac{1}{\delta_0}$ and frequency is held constant, should produce a curve which approaches a value of $a_3\lambda$ asymptotically with increasing tube diameter. Fig. 26 is such a graph determined from experimental data for an initial peak-to-peak pressure of approximately 0.15 atmospheres and a frequency of approximately 800 cps. The values of slopes determined by Werth [4] for 1 inch and 1 1/2 inches tubes are plotted in Fig. 26 for general interest and correlation of data. The curve gives the appearance of asymptotically approaching some value of slope between 0.55 and 0.60. This is in good agreement with Rudnick's theory if the correction proposed by Fay [8] is used. Theory then predicts a value of

$$a_3\lambda = \frac{\gamma+1}{3\gamma} = 0.571 \text{ for air}$$

The apparent agreement of experiment with theory as to the value a_3 makes possible a further comparison of the experimental data with Rudnick's theory predicting the combined effects of attenuation due to shock characteristics and wall effects. From equation (8) it can be seen that if the quantity $\ln(\frac{1}{\delta} + \frac{a_3}{a_2})$ is plotted against X a straight line with slope equal to a_2 would be obtained. It is necessary to use a theoretically determined value of a_2 in the logarithmic term in this procedure to check experimental data against theory. Figs. 27, 28 and 29, in which this procedure is used, show agreement between theory and experimental data. If, however, an attempt is made to determine an experimental value of a_2 by successive approximation methods, the data can be made to fit a considerable range of experimental values of a_2. This is shown in Fig. 30 where a single set of data can be made to give experimental values of .010 and .015 for a_2. Thus, no conclusions can be drawn from this method of analysis.

A final method of presenting experimental data is shown in Figs. 31 and 32. If the values of peak-to-peak pressure for two sets of data of same frequency and tube diameter are such that the reference point pressure of the one set of data is just slightly greater than the end value of the pressure of the other, it is possible to fit the two sets of data together and effectively produce a single run over approximately twice the length of the propagation tube. This is accomplished in Figs. 31 and 32. Also plotted on the graphs are the theoretically

computed curves using equation (6). Good agreement between theory and experimental data is seen.

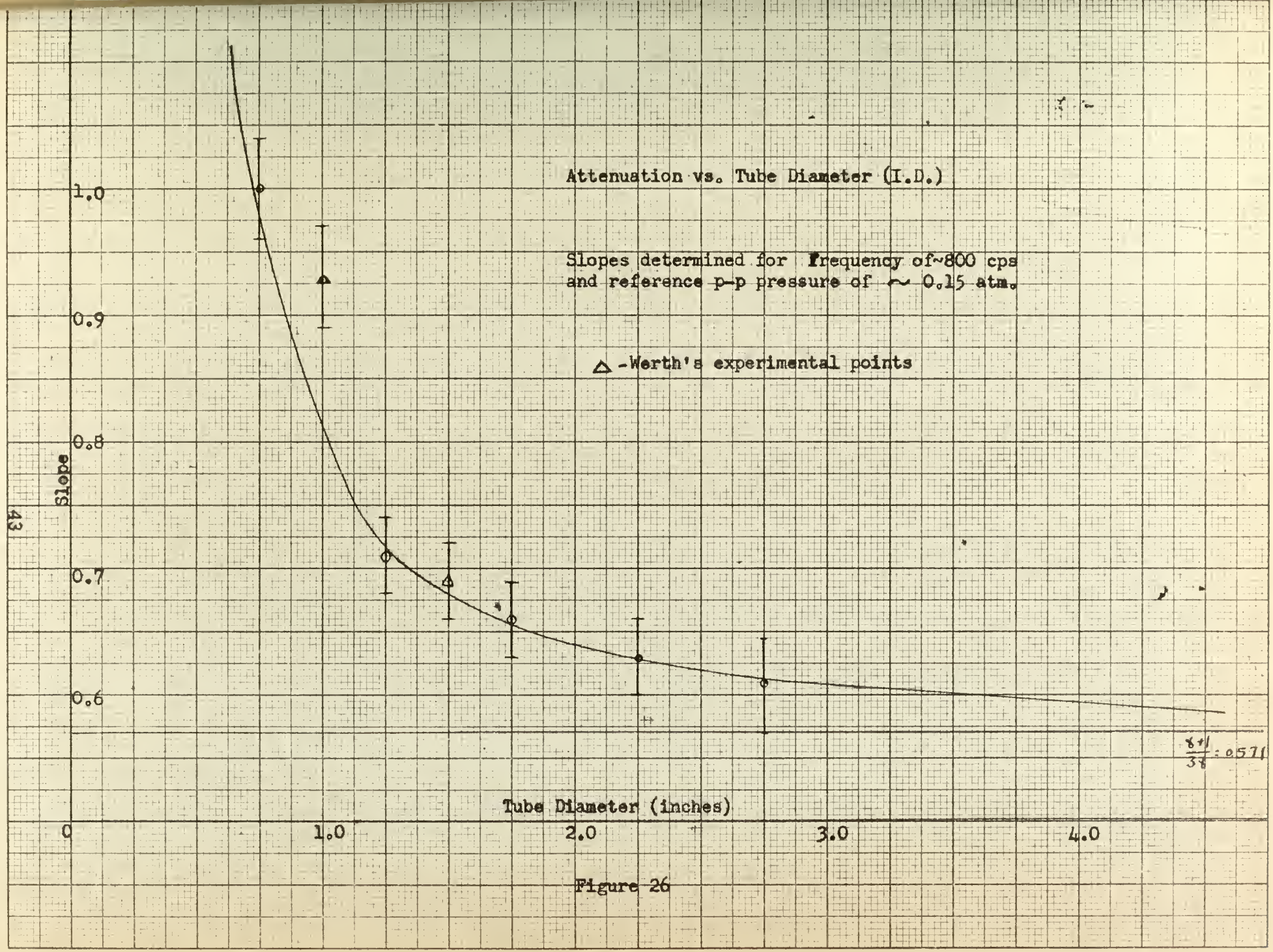
Attenuation vs. Tube Diameter (I.D.)
Slopes determined for frequency of~800 cps
and reference p-p pressure of ~ 0.15 atm.
△ -Werth's experimental points
1.0
0.9
0.8
0.7
0.6
Slope
Tube Diameter (inches)
0
1.0
2.0
3.0
4.0

Figure 26

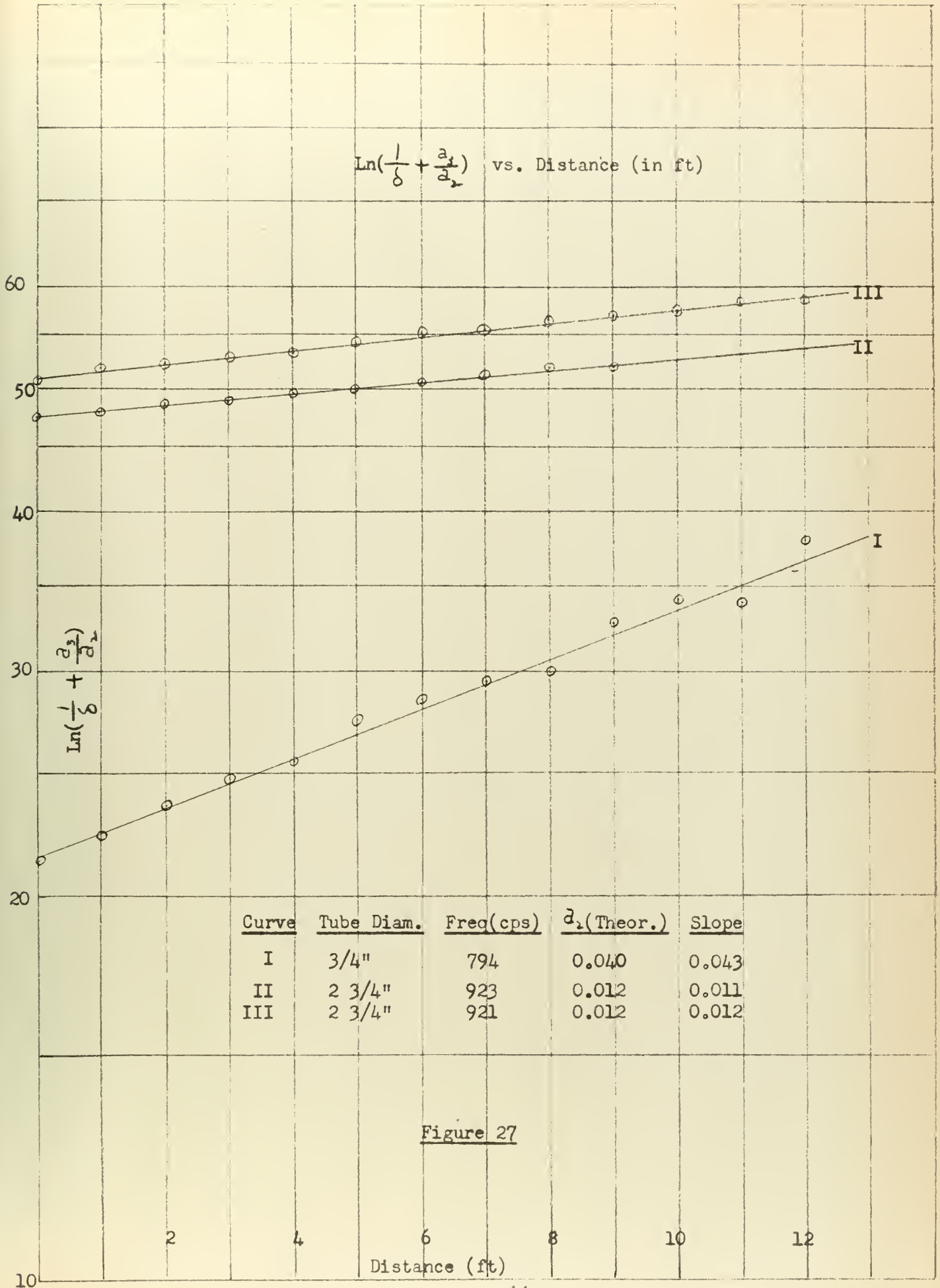

Curve	Tube Diam.	Freq(cps)	a_1(Theor.)	Slope
I	3/4"	794	0.040	0.043
II	2 3/4"	923	0.012	0.011
III	2 3/4"	921	0.012	0.012

Figure 27

$\text{Ln}(\frac{1}{\delta} + \frac{a_2}{a_1})$ vs. Distance (ft)

Curve	Tube Diam.	Freq(cps)	a_2 (Theor.)	Slope
I	$1\frac{1}{4}$"	684	0.021	0.018
II	$1\frac{1}{4}$"	684	0.021	0.020
III	1 3/2"	721	0.016	0.014
IV	2 3/4"	583	0.010	0.011

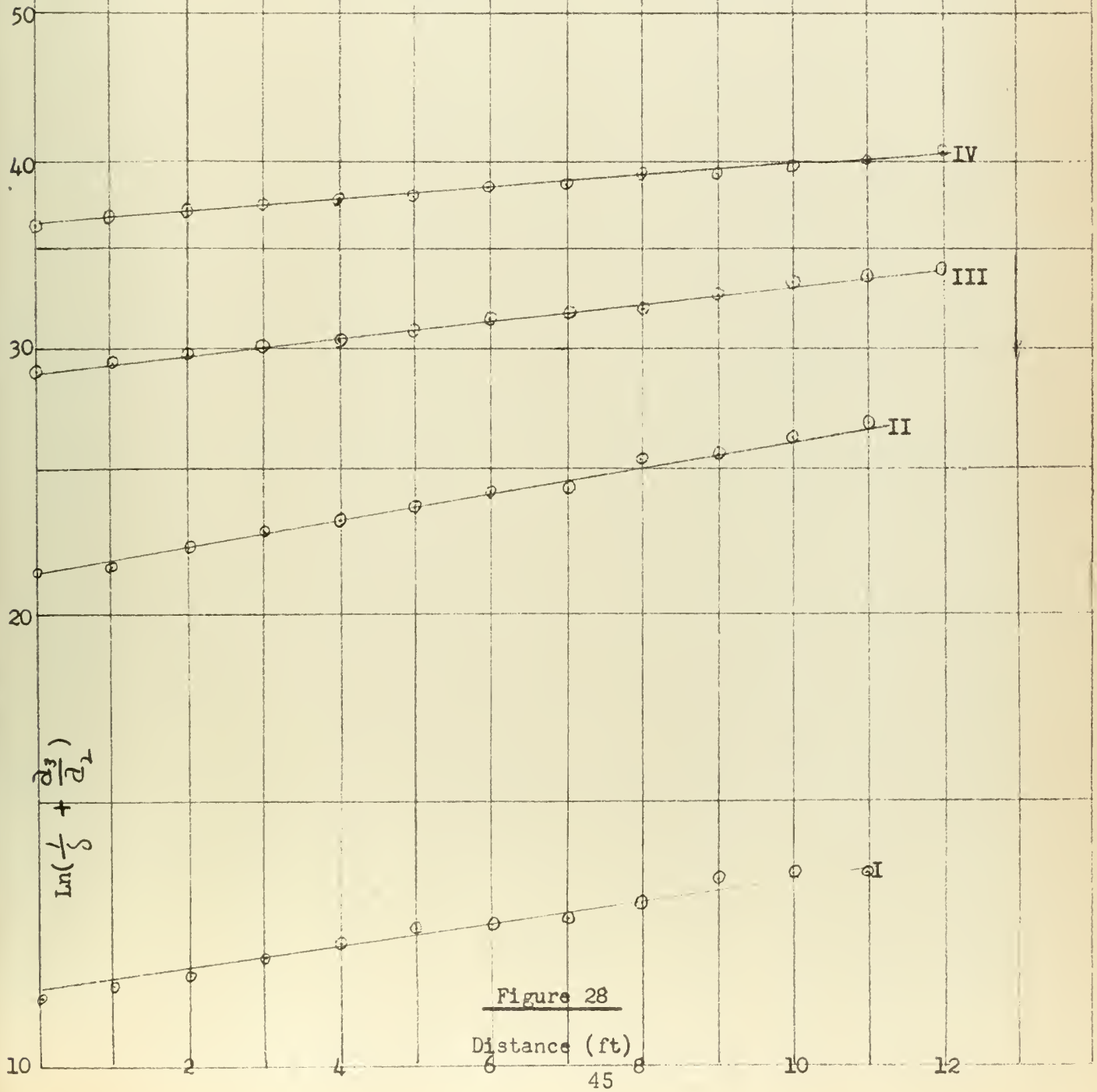

Figure 28

$\text{Ln}\left(\frac{1}{\delta} + \frac{a_1}{a_2}\right)$ vs. Distance(ft)

Curve	Tube Diam.	Freq(cps)	a_2(Theor.)	Slope
I	3/4"	583	0.034	0.022
II	3/4"	690	0.036	0.027
III	1¼"	814	0.024	0.021
IV	2 3/4"	505	0.0087	0.0072
V	2½"	855	0.014	0.012

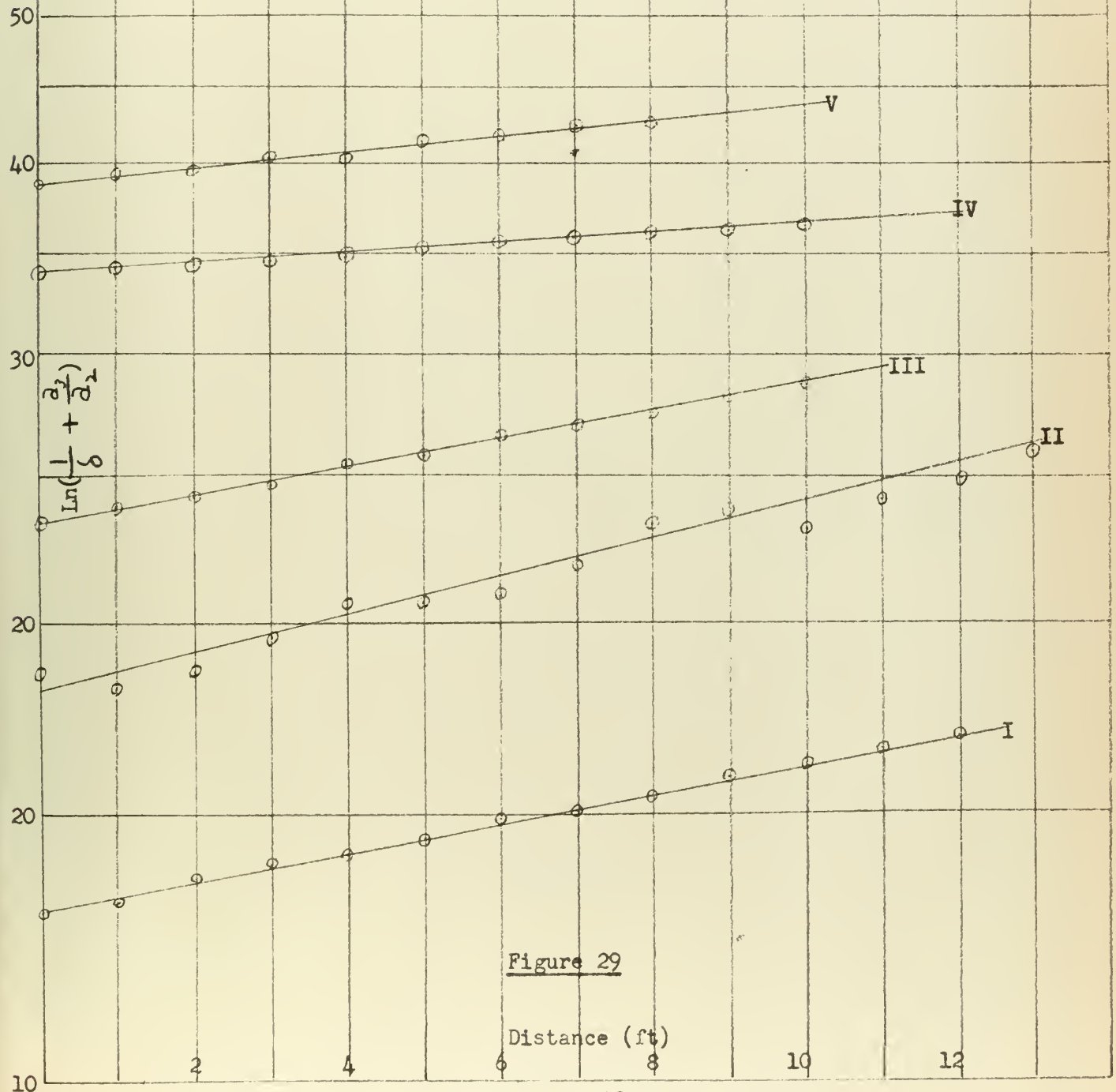

Figure 29

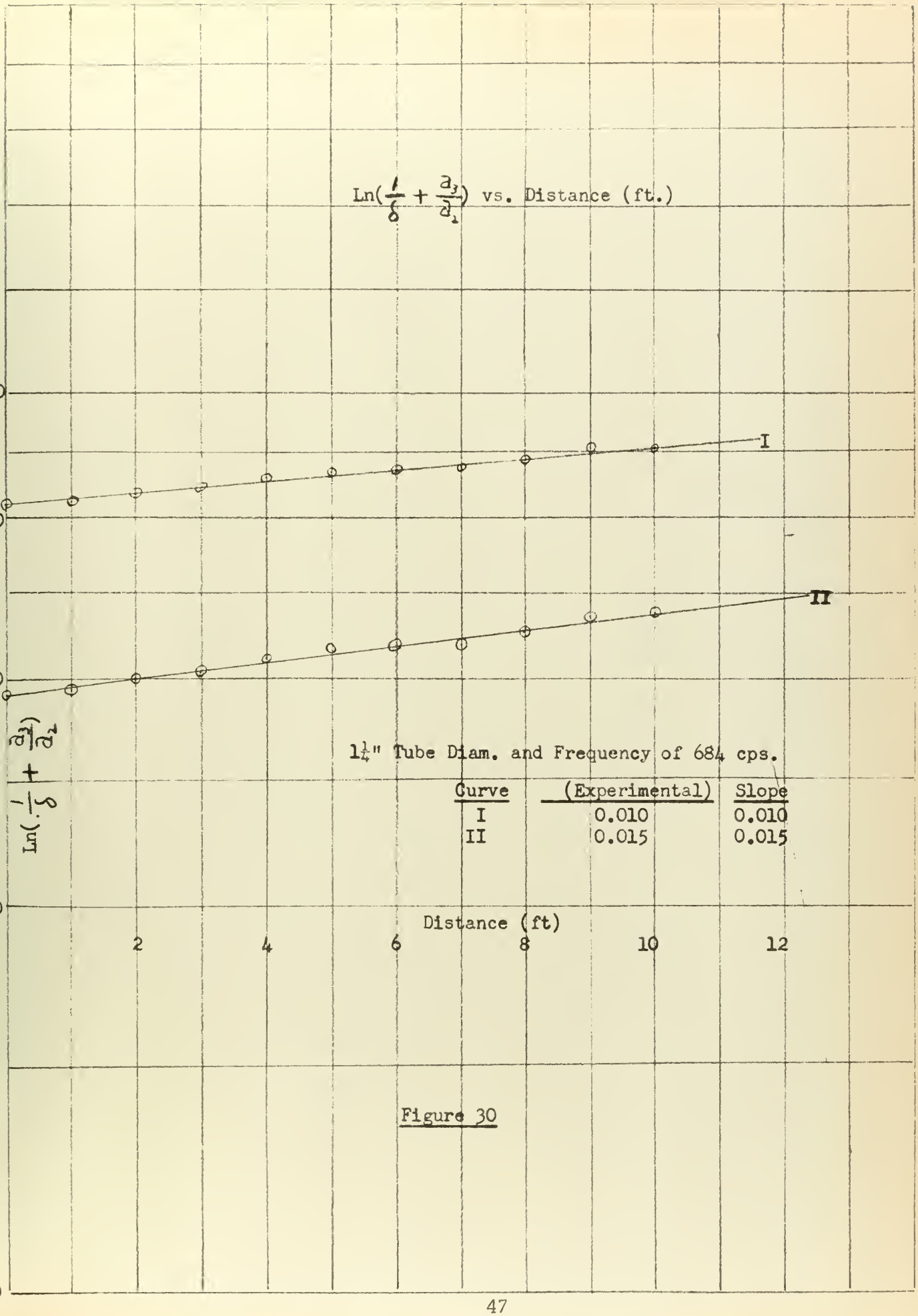
$\text{Ln}\left(\frac{1}{\delta} + \frac{a_3}{a_2}\right)$ vs. Distance (ft.)
50
40
30
20
10
I
II
$\text{Ln}\left(\frac{1}{\delta} + \frac{a_3}{a_2}\right)$
$1\frac{1}{4}$" Tube Diam. and Frequency of 684 cps.
Curve (Experimental) Slope
I 0.010 0.010
II 0.015 0.015
Distance (ft)
2
4
6
8
10
12

Figure 30

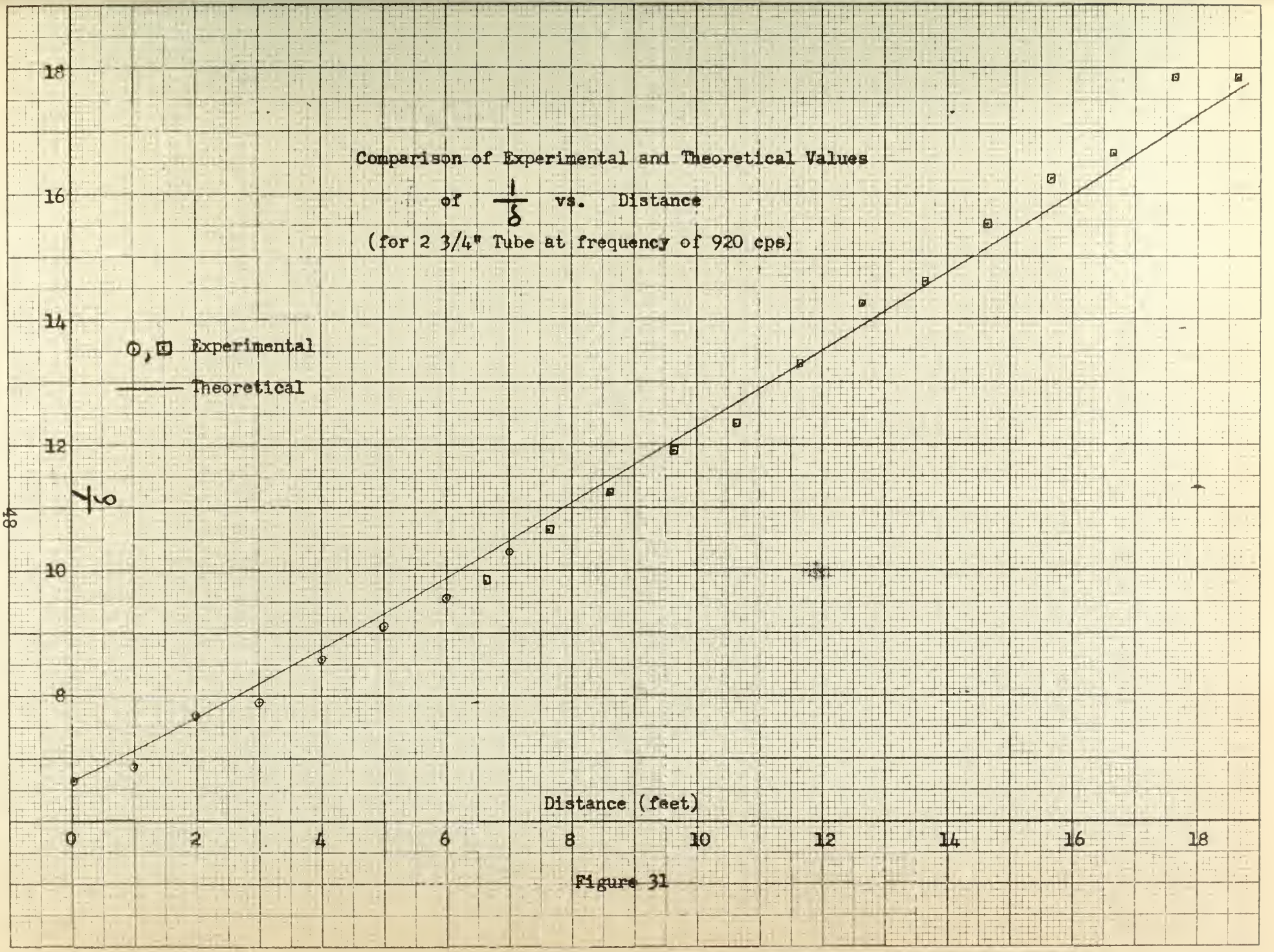
Comparison of Experimental and Theoretical Values
of 1/δ vs. Distance
(for 2 3/4" Tube at frequency of 920 cps)
⊙, ⊡ Experimental
——— Theoretical
1/δ
Distance (feet)
0
2
4
6
8
10
12
14
16
18

Figure 31

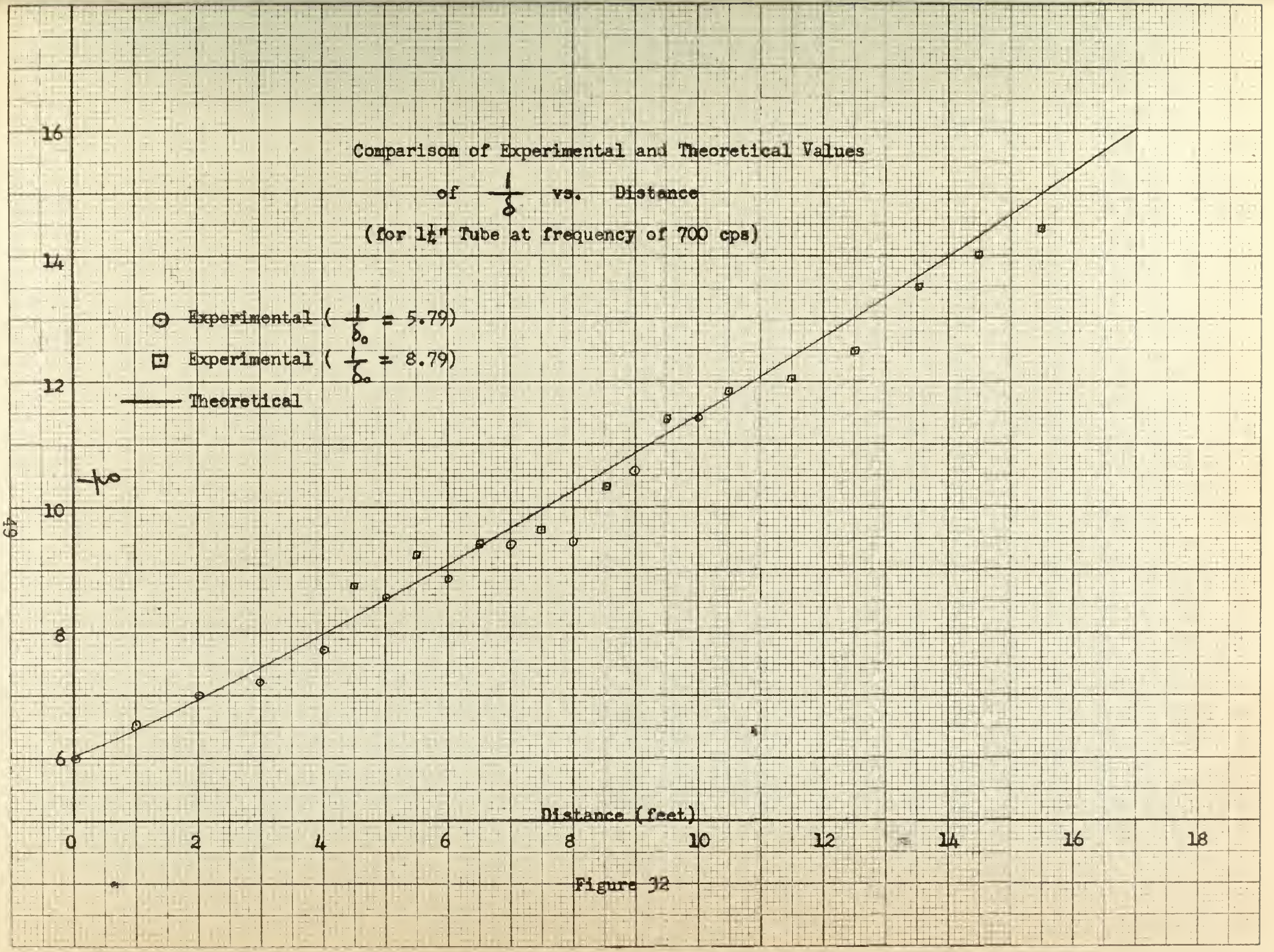
Comparison of Experimental and Theoretical Values
of 1/δ vs. Distance
(for 1½" Tube at frequency of 700 cps)
Experimental (1/δ₀ = 5.79)
Experimental (1/δ₀ = 8.79)
Theoretical
1/δ
Distance (feet)
0
2
4
6
8
10
12
14
16
18
6
8
10
12
14
16

Figure 32

11. Experimental errors.

An error of 10-15% in the measurement of the peak-to-peak pressure swing (and also $\frac{1}{\delta_0}$) at the reference point is estimated. The estimate includes expected error in the absolute calibration of the microphone and probe adapter system plus the error in method of measurement of the peak-to-peak pressure swing as described in Section 7. The differences in peak-to-peak pressures along the propagation tubes were reproducible to within 0.1 db. Errors in evaluation of slopes of $\frac{1}{\delta}$ vs. $\frac{x}{\lambda}$ and $\ln(\frac{1}{\delta} + \frac{a_3}{a_2})$ vs. x vary from 3% to 10%, depending on the magnitude of the standing wave present at the particular frequency and pressure. In general, standing waves were most notable in the 3/4 inch and 2 1/4 inches tubes. Error in frequency measurement was negligible. Intensity of the input signal was held constant during a run to within 0.1 db.

12. Conclusions.

Within the range of pressures and frequencies used in this investigation experimental evidence is presented in support of Fay's theory [8] and of Rudnick's theory for the attenuation of repeated shock waves in tubes when the shock characteristic term is corrected to agree with Fay's analysis. There is some agreement between experimental data and the modified equation

$$\frac{1}{\delta} - \frac{1}{\delta_0} = \left(\frac{a_3}{a_2} + \frac{1}{\delta_0}\right)\left(e^{a_2 x} - 1\right)$$

where

$$a_3 = \frac{\gamma+1}{3\gamma\lambda}$$

but data is not extensive enough to determine an experimental value for a_2.

BIBLIOGRAPHY

1. Report No. 49, Final Report on the High Amplitude Sound Abatement Research Program for the Office of Naval Research, Contract N8 onr 70502. Soundrive Engine Co., Los Angeles, Calif., 1953.

2. I. Rudnick, Report No. 42, Technical Report No. 1 on the High Amplitude Sound Abatement Research Program for the Office of Naval Research, Contract N8 onr 70502. Soundrive Engine Co., Los Angeles, Calif., 1952.

3. I. Rudnick, Report No. 48, Technical Report No. 3 on the High Amplitude Sound Abatement Research Program for the Office of Naval Research, Contract N8 onr 70502. Soundrive Engine Co., Los Angeles, Calif., 1953.

4. Glen C. Werth, J. Acoust. Soc. Am. 26, 59 (1954).

5. O. B. Wilson, Jr., and David A. Bies, Report No. 79, Technical Note on Studies of Very High Amplitude Sound, Contract AF 18(600)-495. Soundrive Engine Co., Los Angeles, Calif., 1954.

6. Lawrence R. Anderson and Donald J. Mehrtens, Thesis "Attenuation of Repeated Shock Waves in Tubes", U. S. Naval Postgraduate School, Monterey, Calif., 1958.

7. R. D. Fay, J. Acoust. Soc. Am. 2, 222 (1931)

8. R. D. Fay, J. Acoust. Soc. Am. 28, 910 (1956)

APPENDIX I

COMPILATION OF DATA

Frequency (CPS)	P-P Press. (Atm)	$\frac{1}{\delta_0}$	Slope ($\frac{1}{\delta}$ vs. No. of Waves)	a_2 (per Ft.)	Slope ($\ln\left[\frac{1}{\delta}+\frac{a_3}{a_1}\right]$) vs. distance)
		2 3/4" I.D. TUBE			
496	.146	6.34	0.58		
505	.224	3.81	0.54	.0087	.0072
583	.135	6.93	0.60	.010	.011
693	.165	5.42	0.62		
693	.152	6.09	0.61		
693	.124	7.57	0.63		
737	.152	6.09	0.64		
790	.113	8.33	0.73		
790	.152	6.09	0.61		
897	.152	6.09	0.63		
921	.097	9.83	0.84	.012	.012
923	.152	6.09	0.66	.012	.011
		2 1/4" I.D. TUBE			
494	.147	6.29	0.58		
588	.135	6.89	0.65		
655	.198	4.54	0.61		
692	.173	5.29	0.59		
692	.119	7.40	0.58		
753	.163	5.62	0.62		

Frequency (CPS)	P-P Press. (Atm)	$\frac{1}{\delta_o}$	Slope ($\frac{1}{\delta_o}$ vs. No. of Waves)	a_2 (per Ft.)	Slope ($\ln\left[\frac{1}{\delta}+\frac{a_2}{a_1}\right]$) vs. distance)
		2 1/4" I.D. TUBE (Cont'd)			
785	.122	7.67	0.61		
806	.152	6.09	0.63		
855	.146	6.35	0.65	.014	.012
926	.092	9.55	0.95		
		1 3/4" I.D. TUBE			
443	.170	5.37	0.52		
503	.178	5.12	0.61		
721	.131	7.14	0.60	.016	.014
789	.128	7.33	0.66		
912	.107	8.87	0.63		
		1 1/4" I.D. TUBE			
505	.155	5.91	0.64	.019	.014
603	.135	6.89	0.61	.021	.014
661	.155	5.97	0.70	.021	.019
684	.167	5.42	0.71	.022	.020
684	.186	4.86	0.68	.022	.018
684	.157	5.85	0.68	.022	.020
684	.146	6.35	0.71	.022	.020
694	.154	5.97	0.71	.022	.020
700	.108	8.79	0.83	.022	.022

Frequency (CPS)	P-P Press. (Atm)	$\frac{1}{\delta_0}$	Slope ($\frac{1}{\delta}$ vs. No. of Waves)	a_2 (per Ft.)	Slope ($\ln\left[\frac{1}{\delta}+\frac{a_2}{a_1}\right]$) vs. distance)
		1 1/4" I.D. TUBE (Cont'd)			
790	.119	7.90	0.74	.024	.021
797	.154	5.97	0.72	.024	.019
814	.154	5.97	0.74	.024	.021
945	.085	11.2	1.01	.028	.031
		3/4" I.D. TUBE			
583	.214	4.18	0.62	.034	.022
613	.140	6.64	1.05	---	
690	.112	8.41	1.30	.036	.027
788	.110	8.55	1.05		
794	.085	11.19	1.68	.040	.043